blasticidin). These cells were grown in a humidified atmosphere of 5% CO_2/95% air at 37°C.

MTT assay. The cell growth inhibition by chemotherapeutic agents was determined by an MTT assay. Cells counted with a hematocytometer were plated in 96-well flat-bottom multiplates (Nalge Nunc International Corp., Rochester, NY, USA) in 100 µl of medium and incubated overnight to permit cell attachment. The medium was then removed from each well and replaced with 100 µl medium containing the drugs for the indicated time. After 72 h, 10 µg of MTT in 10 µl PBS was added to each well, and incubation was continued for an additional 4 h. Thereafter, 100 µl of 0.04 N HCl in 2-propanol was added, and the multiplates were incubated overnight to solubilize the MTT formazan crystal. The absorbance of each well was measured at 570 nm wavelength (reference 650 nm) using a Tecan Sunrise scanning multiwell spectrometer (Tecan Japan Co., Ltd., Kanagawa, Japan). Each experiment was performed in triplicate for each drug concentration and was independently performed three times.

Immunoprecipitation and western blot analysis. Cells were incubated in 6-well tissue culture plates overnight and washed with ice-cold PBS and lysed in lysis buffer [1% NP-40, 0.25% sodium deoxycholate, 150 mM NaCl, pH 7.4, 50 mM Tris-HCl, 1 mM EDTA, 1 mM NaF, 1 mM sodium orthovanadate (Na_3VO_4)] including 1 mM phenylmethylsulfonyl fluoride, 1 µg/ml leupeptin, 1 µg/ml aprotinin, and 1 µg/ml pepstatin. After 5 min on ice, lysates were centrifuged at 13,000 x g for 10 min at 4°C, and the supernatant was then collected. Protein was measured using the Bio-Rad Protein Assay reagent (Bio-Rad Laboratories, Hercules, CA, USA), and protein lysates containing 20 µg of total cellular protein or immunoprecipitates with the indicated antibodies were subjected to discontinuous sodium dodecyl sulfate-polyacrylamide gel electrophoresis (SDS-PAGE).

Proteins were electrotransferred to a polyvinylidene fluoride (PVDF) membrane (GE Healthcare Japan, Tokyo, Japan) for 60 min at 4°C at 100 V. Non-specific binding was blocked by incubation with 5% non-fat milk in Tris-buffered saline containing 0.1% Tween-20 (TBST) for 1 h at room temperature. After blocking, the membrane was incubated in primary antibody (1X PBST containing 1% milk, 1:2,000) overnight at 4°C. The membrane was then washed three times with PBST. The immunoblots were incubated for 1 h in a 1:10,000 dilution of goat anti-rabbit or anti-mouse IgG coupled with horseradish peroxidase as a secondary antibody (GE Healthcare Japan) in TBST containing 1% milk.

Finally, each protein was detected using an enhanced chemiluminescence detection system (ECL prime) and captured with an ImageQuant LAS 400 (both from GE Healthcare Japan). The antibody against EGFR was purchased from Santa Cruz Biotechnology, Inc. (Santa Cruz, CA, USA). Anti-phosphotyrosine antibody (4G10) was purchased from Merck Millipore (Darmstadt, Germany), and anti-β-actin antibody was purchased from Sigma-Aldrich Japan (Tokyo, Japan).

Assessment of combination effect. A combination index (CI) was calculated using the Chou-Talalay method (25) and used to evaluate the combination effect of the two drugs. The CI quantitatively depicts synergism (CI<1), addictive effect (CI=1), and antagonism (CI>1).

Results

The characteristics of patients and efficacy of VNR + DIF and platinum-based chemotherapy. A total of 39 patients were included in this retrospective study. The ages of the 39 patients ranged from 35 to 84 years (median age, 65 years), with 16 males (41.0%) and 23 females (59%). All tumors were adenocarcinomas, and 31 patients had stage IV disease (79.5%). Seven patients received gefitinib prior to cytotoxic chemotherapy.

At the first cytotoxic chemotherapy, 24 patients received VNR + DIF chemotherapy (VNR + UFT, n=5; VNR + S-1, n=19) and the other 15 patients received platinum-based chemotherapy. Of the 15 patients in the platinum group, eight patients received CDDP-based chemotherapy (CDDP + gemcitabine, n=4; CDDP + docetaxel, n=4), and the seven others received carboplatin-based chemotherapy (carboplatin + paclitaxel, n=5; carboplatin + pemetrexed, n=1; carboplatin + gemcitabine, n=1).

Table I shows the patient characteristics according to the first-line chemotherapy regimen (VNR + DIF vs. platinum). There was no significant difference between the two regimen groups with regard to age, gender, disease stage, smoking status, EGFR mutation type, Eastern Cooperative Oncology Group (ECOG) performance status (PS), and chemotherapy line. As a later line of cytotoxic chemotherapy, seven (29.2%) patients in the VNR + DIF group received platinum-based chemotherapy, and four (26.7%) patents in the platinum group received VNR + DIF treatment.

Both the objective response rate (ORR) and the disease control rate (DCR) of the VNR + DIF patients were favorable compared with those of the platinum group, although the differences were not significant (54.2 vs. 42.9%, p=0.74 and 87.5 vs. 71.4%, p=0.39; Table II). Fig. 1 shows the Kaplan-Meier curves for PFS in the VNR + DIF and platinum groups. The median PFS of the VNR + DIF group was significantly longer than that of the platinum group (7.4 vs. 3.7 months, p=0.02). The median OS was not significantly different between the two groups (36.6 vs. 35.4 months, p=0.34; Table II).

The cell growth inhibition and effect of VNR, CDDP and 5-FU on EGFR phosphorylation in PC9 cells. Based on the results of the retrospective study, we speculated that VNR or DIF may have an effect on EGFR activity. To address this speculation, we performed *in vitro* experiments using PC9 cells harboring an active form of *EGFR* mutation.

We first evaluated the sensitivity of PC9 cells to VNR, 5-FU, and CDDP. The half-life of VNR in plasma after intravenous injection is ~20 h (26), and CDDP is almost completely eliminated within 24 h from plasma (27). In previous studies, DIF was orally administered to patients for 5 days in the combination of VNR + DIF (19,20), and the 5-FU concentration in plasma stayed roughly constant during an oral intake of DIF (28,29). We therefore exposed PC9 cells to VNR, CDDP and 5-FU for 24, 24 and 72 h, respectively, and 72 h after the start of drug exposure, we performed an MTT assay to evaluate the inhibition of cell proliferation. The concentration

Table I. Characteristics of the 39 lung adenocarcinoma patients harboring *EGFR* mutations.

	VNR + DIF (n=24)	Platinum (n=15)	P-value
Age (years)			0.31[a]
Median (range)	66.5 (50–84)	64 (35–74)	
Sex			0.92[b]
Male	10	6	
Female	14	9	
Disease stage			0.84[c]
IIIA	1	0	
IIIB	3	2	
IV	19	12	
Recurrence	1	1	
Histology			
Adenocarcinoma	24	15	
Smoking status			0.74[c]
Current	3	3	
Former	5	4	
Never	16	8	
EGFR mutation type			0.41[c]
Exon 19 deletion	13	6	
Exon 21 point mutation	7	7	
Minor mutation	2	0	
Unknown	2	2	
Performance status			0.44[c]
0	14	8	
1	10	6	
2	0	1	
Chemotherapy line			0.87[b]
First-line	20	12	
Second-line (gefitinib as first-line)	4	3	

[a]Mann-Whitney test, [b]Fisher's exact test and [c]χ^2 test. EGFR, epidermal growth factor receptor; VNR, vinorelbine; DIF, dihydropyrimidine dehydrogenase-inhibitory fluoropyrimidine.

Table II. Comparison of efficacy parameters between the combination of VNR + DIF and platinum-based chemotherapy.

Confidence interval (95%)	VNR + DIF (n=24)	Platinum (n=15)	P-value
ORR	54.2 (32.0-76.4)	42.9 (29.6-56.1)	0.74[a]
DCR	87.5 (80.7-94.3)	71.4 (59.4-83.5)	0.39[a]
mPFS (months)	7.4 (6.2-8.7)	3.7 (2.9-4.6)	0.02[b]
mOS (months)	36.6 (27.2-46.0)	35.4 (31.0-39.7)	0.34[b]

[a]Fisher's exact test and [b]log-rank test. VNR, vinorelbine; DIF, dihydropyrimidine dehydrogenase-inhibitory fluoropyrimidine; ORR, objective response rate; DCR, disease control rate; mPFS, median progression-free survival; mOS, median overall survival.

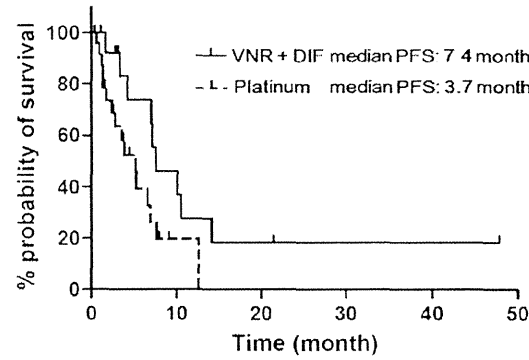

Figure 1. Kaplan-Meier curves of the progression-free survival (PFS) of the patients who received vinorelbine (VNR) + dehydrogenase-inhibitory fluoropyrimidine (DIF) chemotherapy (n=24) or platinum-based chemotherapy (n=15).

of VNR producing a 50% inhibition of cell growth (IC_{50}) was 8.1 nM, that of CDDP was 0.59 μM, and that of 5-FU was 13.8 μM (Fig. 2), and these are clinically achievable concentrations (26-29).

We evaluated the phosphorylation of EGFR after the treatment with each drug at the concentrations up to ~2-fold higher than the IC_{50}. After the treatment with a 10 nM or higher concentration of VNR for 24 h, the phosphorylation of EGFR was clearly decreased. In the PC9 cells, this EGFR dephosphorylation induced by VNR appeared 12-24 h after the start of the exposure to 20 nM VNR (Fig. 3A), whereas such dephosphorylation of EGFR was not detected in the 24-h treatment with 5-FU or CDDP at the concentrations tested (Fig. 3B and C).

The cell growth inhibition and effects of gefitinib, VNR, CDDP and 5-FU on EGFR phosphorylation in 1BR3-LR cells. To elucidate whether the suppression of EGFR phosphorylation induced by VNR functions as an anti-proliferative mechanism of VNR, we used 1BR3 cells (in which EGFR is not expressed), stably transfected with the L858R mutant *EGFR* (1BR3-LR).

We determined the effects of gefitinib, VNR, CDDP and 5-FU on EGFR phosphorylation in 1BR3-LR cells. As shown in Fig. 4A, the treatment with 10 nM VNR for 24 h suppressed EGFR phosphorylation as well as gefitinib did, a selective EGFR-TKI in 1BR3-LR cells. Similar to the PC9 cells, neither CDDP nor 5-FU induced the dephosphorylation of EGFR.

We evaluated the cell growth inhibition by these drugs in 1BR3-LR cells. In 1BR3-LR cells cultured in 10% FBS-containing medium, gefitinib slightly promoted cell growth, although it effectively suppressed EGFR phosphorylation. Gefitinib inhibited the cell growth concentration dependently in the medium containing 0.5% FBS (Fig. 4B), indicating that

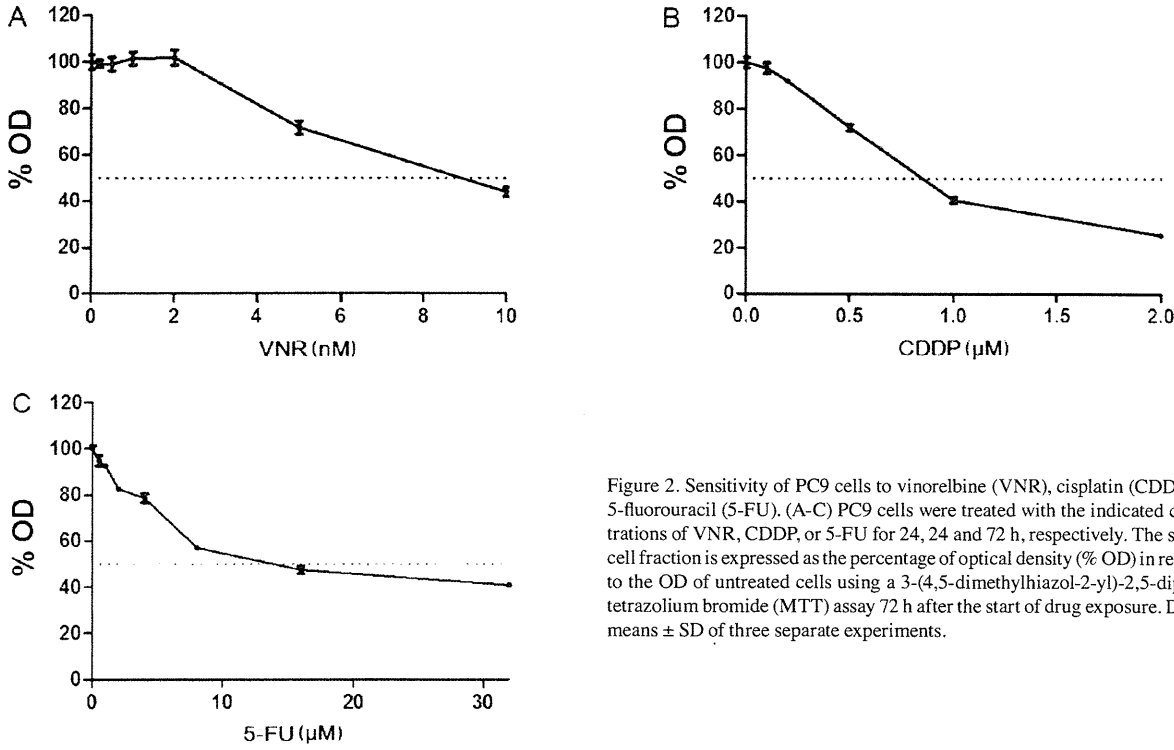

Figure 2. Sensitivity of PC9 cells to vinorelbine (VNR), cisplatin (CDDP), and 5-fluorouracil (5-FU). (A-C) PC9 cells were treated with the indicated concentrations of VNR, CDDP, or 5-FU for 24, 24 and 72 h, respectively. The survival cell fraction is expressed as the percentage of optical density (% OD) in reference to the OD of untreated cells using a 3-(4,5-dimethylhiazol-2-yl)-2,5-diphenyltetrazolium bromide (MTT) assay 72 h after the start of drug exposure. Data are means ± SD of three separate experiments.

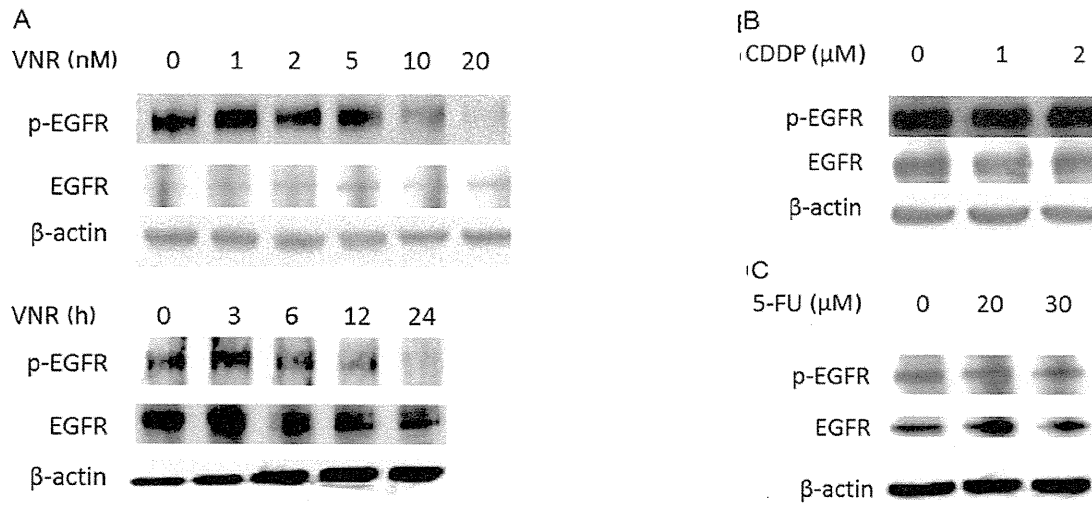

Figure 3. Effects of vinorelbine (VNR), cisplatin (CDDP), and 5-fluorouracil (5-FU) on epidermal growth factor receptor (EGFR) phosphorylation in PC9 cells. (A) PC9 cells were treated with the indicated concentrations of VNR for 24 h (upper panels), or 20 nM VNR for the indicated time (lower panels). Total cellular protein (1 mg) from cell lysate was immunoprecipitated using anti-EGFR antibody and subjected to a western blot analysis with anti-phosphotyrosine (p-EGFR, upper panel), and the membrane was stripped of bound antibodies and re-probed with anti-EGFR antibody (middle panel). Total cellular protein (20 μg) of the same lysate was subjected to a western blot analysis with β-actin (lower panel). (B and C) PC9 cells were treated with the indicated concentrations of CDDP or 5-FU for 24 h and processed as described above.

the proliferation or survival of 1BR3-LR cells is dependent on EGFR-mediated signaling in low-serum condition.

We compared the growth inhibitory activities of VNR, 5-FU, and CDDP in 1BR3-LR cells between normal (10%) and low (0.5%) serum conditions, and we found that the cell growth inhibition by VNR was enhanced in the low-serum condition compared to that in the normal-serum condition (Fig. 4C). The sensitivity of 1BR3-LR cells to CDDP did not clearly differ by serum concentration (Fig. 4D). In the low-serum condition, 1BR3-LR cells tended to be resistant to 5-FU-induced cell growth inhibition (Fig. 4E).

The effect of Na_3VO_4 on EGFR phosphorylation and gefitinib- and VNR-induced cell growth inhibition. To further test whether the EGFR dephosphorylation induced by VNR was related to anti-proliferative effect of VNR, we tested

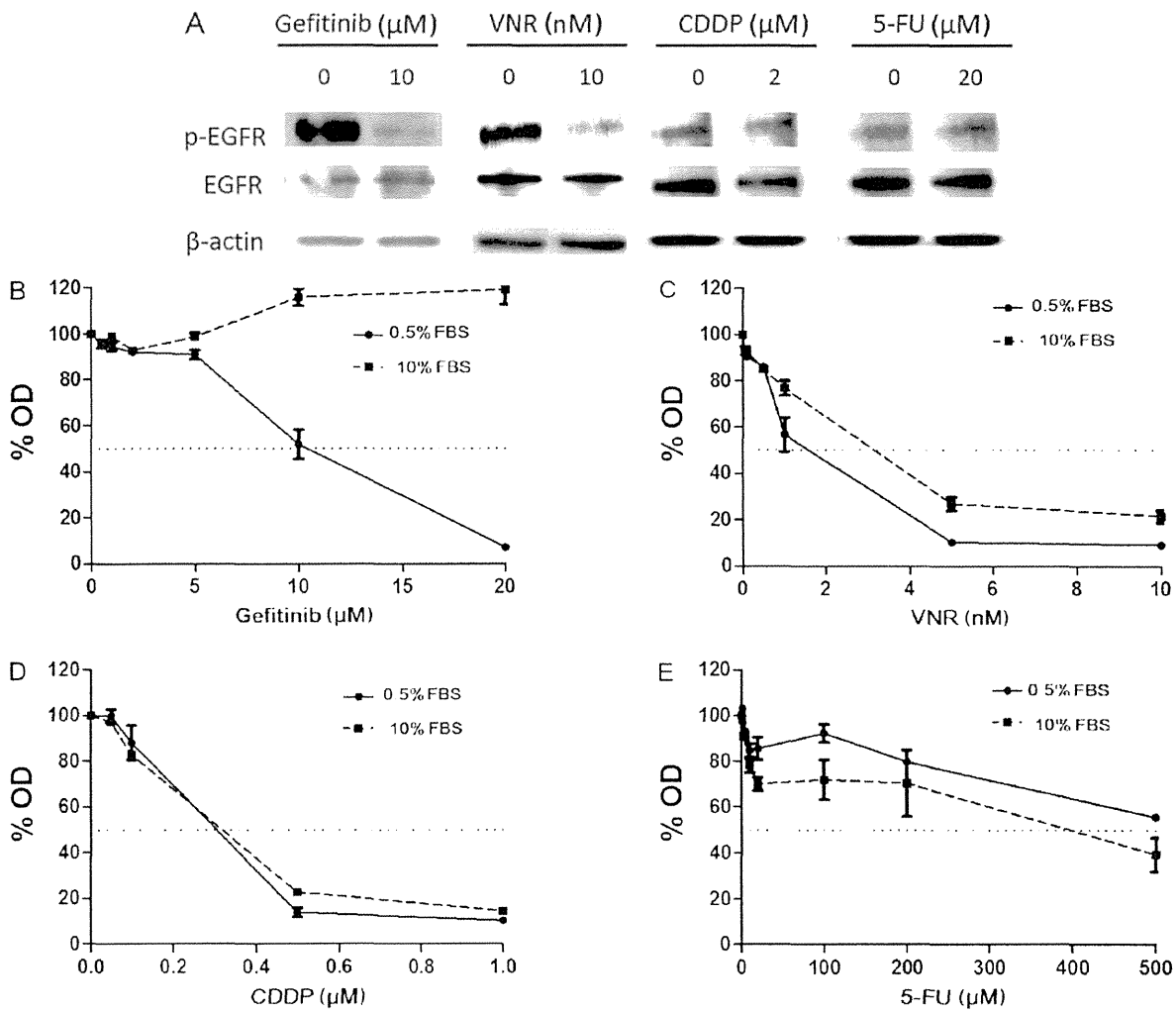

Figure 4. Effects of vinorelbine (VNR), cisplatin (CDDP), and 5-fluorouracil (5-FU) on epidermal growth factor receptor (EGFR) phosphorylation and cell growth inhibition in 1BR3-LR cells. (A) 1BR3-LR cells were treated with the indicated concentrations of gefitinib, VNR, CDDP, or 5-FU for 24 h. Total cellular protein (1 mg) from cell lysate was immunoprecipitated using anti-EGFR antibody and subjected to a western blot analysis with anti-phosphotyrosine (p-EGFR, upper panel), and the membrane was stripped of bound antibodies and re-probed with anti-EGFR antibody (middle panel). Total cellular protein (20 μg) of the same lysate was subjected to a western blot analysis with β-actin (lower panel). (B-E) 1BR3-LR cells were treated with the indicated concentrations of gefitinib, VNR, CDDP, or 5-FU for 72 h in the medium containing 10% (solid line) or 0.5% (dotted line) fetal bovine serum (FBS). The survival cell fraction is expressed as the percentage of optical density (% OD) in reference to the OD of the untreated cells in an 3-(4,5-dimethylhiazol-2-yl)-2,5-diphenyltetrazolium bromide (MTT) assay. Data are presented as means ± SD of three separate experiments.

whether Na_3VO_4, an inhibitor of protein tyrosine phosphatases, can interfere with the gefitinib- or VNR-induced dephosphorylation of EGFR and affect the cell growth inhibition by gefitinib or VNR in PC9 cells. We treated PC9 cells with 50 nM gefitinib or 20 nM VNR in the presence or absence of 50 μM Na_3VO_4 for 24 h and then evaluated the EGFR phosphorylation. The EGFR dephosphorylation caused by gefitinib or VNR was clearly inhibited in the presence of Na_3VO_4 (Fig. 5A and B).

The cell growth inhibition of PC9 cells by gefitinib or VNR was compared in the presence or absence of Na_3VO_4. As shown in Fig. 5C and D, the cell growth inhibitory activity of both gefitinib and VNR was greatly interfered with by Na_3VO_4.

Synergistic cell growth inhibition by the combination of gefitinib or VNR with 5-FU in PC9 cells. In our previous study, the combination treatment of VNR and subsequent 5-FU synergistically inhibited cell growth in three NSCLC cell lines (18). In the present study, to reproduce this synergism and to clarify whether EGFR suppression by VNR is related to this interaction, we evaluated the combination effects using the CI and the simultaneous combination of gefitinib and 5-FU, or the sequential treatment of VNR followed by 5-FU. Since gefitinib suppressed EGFR activity within 1 h *in vitro* (6), gefitinib and 5-FU were combined simultaneously.

We treated PC9 cells with the indicated concentrations of gefitinib + 5-FU for 72 h or VNR for 24 h and 5-FU for the following 72 h, and we calculated the CI (Fig. 6). As shown in the Fig., the CI values for the combination of gefitinib and 5-FU were all <1.0, indicating that this simultaneous combination showed synergistic cell growth inhibitory activity against PC9 cells. Similar results were achieved for sequential exposure to VNR followed by 5-FU with CI<0.3, which implied strong synergism (Fig. 6B).

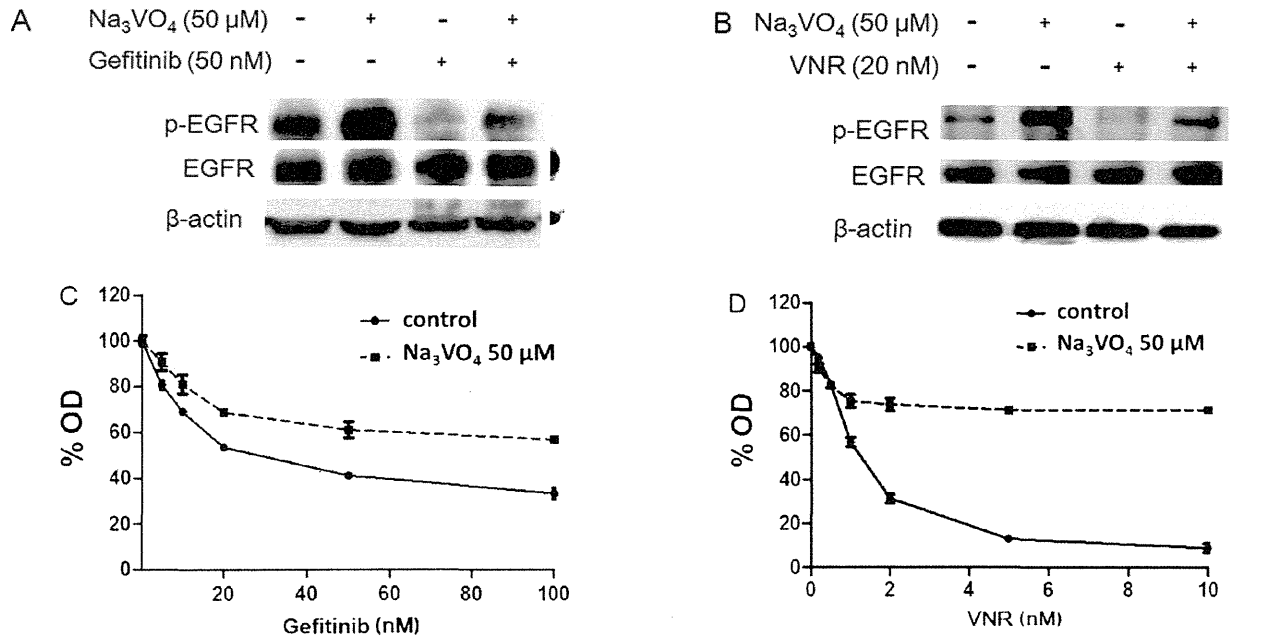

Figure 5. Effects of sodium orthovanadate (Na_3VO_4) on epidermal growth factor receptor (EGFR) phosphorylation and the cell growth inhibition by gefitinib or vinorelbine (VNR) in PC9 cells. (A and B) PC9 cells were treated with 50 nM gefitinib or 20 nM VNR in the presence or absence of 50 μM Na_3VO_4 for 24 h. Total cellular protein (1 mg) from cell lysate was immunoprecipitated using anti-EGFR antibody and subjected to a western blot analysis with anti-phosphotyrosine (p-EGFR, upper panel), and the membrane was stripped of bound antibodies and re-probed with anti-EGFR antibody (middle panel). Total cellular protein (20 μg) of the same lysate was subjected to a western blot analysis with β-actin (lower panel). (C and D) PC9 cells were treated with the indicated concentrations of gefitinib or VNR in the presence or absence of 50 μM Na_3VO_4 for 72 h. The survival cell fraction is expressed as the % OD in reference to the OD of the untreated cells in an 3-(4,5-dimethylhiazol-2-yl)-2,5-diphenyltetrazolium bromide (MTT) assay. Data are means ± SD of three separate experiments.

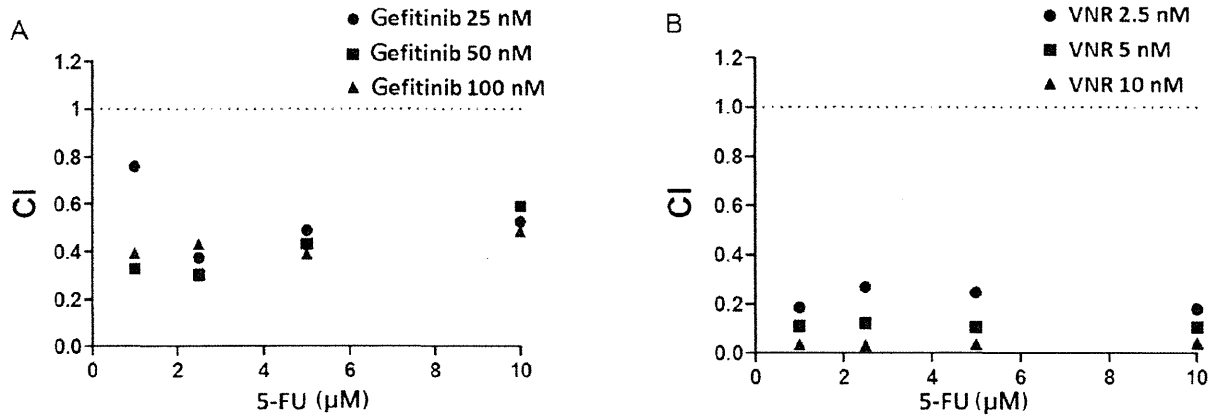

Figure 6. The synergistic cell growth inhibition by the combination of gefitinib or vinorelbine (VNR) with 5-fluorouracil (5-FU) in PC9 cells. (A) PC9 cells were treated with either a single agent or the simultaneous combination of 5-FU and gefitinib for 72 h. (B) PC9 cells were treated with either a single agent or the sequential combination of VNR for 24 h and 5-FU for the next 72 h. The viabilities of the cells were determined in an 3-(4,5-dimethylhiazol-2-yl)-2,5-diphenyltetrazolium bromide (MTT) assay. The combination index (CI) for each concentration of 5-FU was calculated by the Chou-Talalay method.

Discussion

The aim of this study was to evaluate whether the combination of VNR + DIF is a more effective treatment compared with the standard platinum-based chemotherapy in *EGFR*-mutated lung adenocarcinoma patients, and then to clarify the underlying mechanism by which VNR + DIF was efficacious in such patients. In the retrospective analysis, the PFS of the patients who received VNR + DIF chemotherapy was longer than that of the patients who received platinum-based chemotherapy. Using mutated EGFR-expressing cells, we found that VNR induced EGFR dephosphorylation and that this effect of VNR may be related to its cell growth inhibitory activity. We propose that EGFR inhibition by VNR may be one of the mechanisms of the synergistic effect by the sequential treatment of VNR and subsequent 5-FU.

In this retrospective study, the characteristics of the patients who received VNR + DIF chemotherapy were not significantly different from those who received platinum-based chemotherapy. Nevertheless, the PFS of the VNR + DIF treatment group was significantly longer than that of the platinum-based chemotherapy group. The RR and DCR values of the VNR + DIF chemotherapy patients also tended to be better than those of the platinum-based chemotherapy patients, although the difference was not significant. These results suggest that the combination of VNR + DIF may be more effective than platinum-based chemotherapy, at least in terms of the antitumor effect in lung adenocarcinomas with EGFR-activating mutations.

Despite the significant difference in PFS, the OS of the present two regimen groups was not significantly different. Over one-quarter of the patients in each group crossed over to the other regimen as a later-line treatment. The comparison of OS was performed between small groups (n=24 for VNR + DIF, n=15 for platinum), and thus the statistical power was low. We suspect that the lack of a significant difference in OS was due to these reasons. In a proportional hazard analysis performed in another study, we found that the application of the VNR + DIF combination but not platinum-based chemotherapy was a significant and independent factor to prolong survival in lung adenocarcinoma patients with *EGFR* mutations (unpublished data). These results suggest that VNR + DIF chemotherapy may be superior to platinum-based chemotherapy in the treatment of lung adenocarcinoma patients with *EGFR* mutations.

To clarify the mechanisms by which VNR + DIF chemotherapy was favorable in the treatment of *EGFR*-mutated lung adenocarcinoma, we focused on the effects of VNR and 5-FU on EGFR phosphorylation. In *EGFR*-mutated PC9 cells, VNR induced EGFR dephosphorylation 12-24 h after drug exposure at the concentration of 10 nM or higher. In the treatment of NSCLC, when 20-30 mg/m^2 of VNR is administered, a VNR concentration >10 nM is maintained in peripheral blood for 12-24 h (26). Thus, an EGFR-dephosphorylating concentration of VNR is clinically achievable.

The sufficiently cell growth-inhibiting and clinically relevant concentration of CDDP and 5-FU (27-29) did not affect the EGFR phosphorylation in PC9 cells. Our observation in terms of EGFR dephosphorylation by VNR is in accord with the result of a previous investigation. Wu *et al* reported that in esophageal cancer cells, the disruption of the microtubule network induced by microtubule-targeting drugs such as docetaxel and vincristine, another vinca-alkaloid, was associated with EGFR dephosphorylation and the subsequent inhibition of Akt and Erk (30). VNR is a semisynthetic vinca-alkaloid, a member of the family of microtubule-targeting drugs. Although the precise mechanism is still unknown, EGFR-suppressing activity may thus be a common property among taxanes and vinca-alkaloids.

To test whether the EGFR dephosphorylation induced by VNR is associated with its anti-proliferative effect, we took advantage of 1BR3-LR cells, which express an active form of EGFR. Parental 1BR3 cells do not express EGFR. Although we observed that 1BR3-LR cells were completely resistant to gefitinib in normal culture medium containing 10% FBS, gefitinib showed cell growth inhibition against 1BR3-LR cells in the medium containing 0.5% FBS. These results indicate that the growth or survival of 1BR3-LR cells is at least partially dependent on EGFR signaling in a low-serum condition.

We also found that the growth inhibition of 1BR3-LR cells by VNR was enhanced in the low-serum condition, although such changes of drug sensitivity were not observed in CDDP- or 5-FU-treated cells. These findings strongly support the interpretation that the enhanced sensitivity to VNR in the low-serum condition is not a non-specific effect but rather is due to the suppression of EGFR signaling, since both gefitinib and VNR (and not CDDP or 5-FU) suppressed EGFR phosphorylation.

This interpretation is further supported by our finding that Na_3VO_4 interfered with the EGFR dephosphorylation induced by gefitinib and VNR, and suppressed the cell growth inhibition by these agents in PC9 cells. Taken together, our results led us to conclude that VNR-induced EGFR dephosphorylation is associated with the anti-proliferative effect of VNR in lung adenocarcinoma cell lines harboring *EGFR* mutations.

We found previously that the combination of VNR followed by 5-FU resulted in synergistic cell growth inhibition in three NSCLC cell lines (18). The synergism was also observed in PC9 cells harboring an *EGFR* mutation with the sequential treatment of VNR and then 5-FU. Therefore, although it still remains to be determined whether the EGFR suppression by VNR itself may lead to a better antitumor effect of VNR in *EGFR*-mutated lung adenocarcinoma, it is possible that this synergism also contributed to the favorable antitumor activity observed in patients treated with VNR + DIF.

In addition, as in an earlier study (31), the simultaneous combination of gefitinib and 5-FU showed synergistic cell growth inhibition in PC9 cells in the present study. Therefore, the synergism of VNR followed by 5-FU may be attributable, at least in part, to the EGFR-suppressing activity of VNR.

The important therapeutic target of 5-FU is thymidylate synthase (TS), and the downregulation of TS would be expected to enhance the cytotoxicity of 5-FU (32). EGFR signal transduction has been shown to be involved in the expression of *TS* genes (33,34), and in our previous study, VNR as well as gefitinib was shown to suppress TS expression (18). Thus, the decrease of TS caused by EGFR suppression may be a common mechanism of the synergism by the combination of VNR or gefitinib with 5-FU.

The identification of activating mutations of the *EGFR* gene in a subset of NSCLC patients led to a change in the treatment of the disease (6), and the presence of *EGFR* mutations is a predictive marker of response to EGFR-TKI (3,4). It has been reported that the effect of cytotoxic chemotherapy is not different between patients with and without *EGFR* mutations (35,36). Thus, the cytotoxic agents for NSCLC patients with *EGFR* mutations are not different from those used for *EGFR* wild-type patients. To our knowledge, there has been no prospective study attempting to identify which agents or combination chemotherapy is specifically effective in *EGFR*-mutated NSCLC.

The identification of such cytotoxic agents or combination chemotherapy is expected to improve the survival of NSCLC

patients harboring *EGFR* mutations. In the present study, we observed favorable PFS by the combination of VNR + DIF and the potential mechanism of this good treatment outcome. We propose that the combination chemotherapy of VNR and DIF can be a promising strategy for NSCLC patients harboring *EGFR* mutations. Since our observations were retrospective and experimental, there are several limitations. To establish the optimal VNR + DIF combination chemotherapy in NSCLC patients with *EGFR* mutations, we are performing a prospective phase II trial of this treatment targeting such patients.

In conclusion, the PFS afforded by the VNR + DIF combination treatment was significantly longer compared to that of platinum-based chemotherapy in lung adenocarcinoma patients with *EGFR* mutations. VNR suppressed EGFR phosphorylation in PC9 cells, and this activity may be related with cell growth inhibition of VNR, and the synergistic cell growth inhibition when VNR was combined with 5-FU. The combination chemotherapy of VNR + DIF may be a promising treatment for NSCLC patients with *EGFR* mutations.

References

1. Schiller JH, Harrington D, Belani CP, *et al*: Comparison of four chemotherapy regimens for advanced non-small-cell lung cancer. N Engl J Med 346: 92-98, 2002.
2. Ohe Y, Ohashi Y, Kubota K, *et al*: Randomized phase III study of cisplatin plus irinotecan versus carboplatin plus paclitaxel, cisplatin plus gemcitabine, and cisplatin plus vinorelbine for advanced non-small-cell lung cancer: Four-Arm Cooperative Study in Japan. Ann Oncol 18: 317-323, 2007.
3. Paez JG, Jänne PA, Lee JC, *et al*: EGFR mutations in lung cancer: correlation with clinical response to gefitinib therapy. Science 304: 1497-1500, 2004.
4. Mitsudomi T and Yatabe Y: Mutations of the epidermal growth factor receptor gene and related genes as determinants of epidermal growth factor receptor tyrosine kinase inhibitors sensitivity in lung cancer. Cancer Sci 98: 1817-1824, 2007.
5. Nana-Sinkam SP and Powell CA: Molecular biology of lung cancer: diagnosis and management of lung cancer, 3rd ed: American College of Chest Physicians evidence-based clinical practice guidelines. Chest 143 (Suppl 5): e30S-e39S, 2013.
6. Lynch TJ, Bell DW, Sordella R, *et al*: Activating mutations in the epidermal growth factor receptor underlying responsiveness of non-small-cell lung cancer to gefitinib. N Engl J Med 350: 2129-2139, 2004.
7. Mitsudomi T, Morita S, Yatabe Y, *et al*: Gefitinib versus cisplatin plus docetaxel in patients with non-small-cell lung cancer harbouring mutations of the epidermal growth factor receptor (WJTOG3405): an open label, randomised phase 3 trial. Lancet Oncol 11: 121-128, 2010.
8. Maemondo M, Inoue A, Kobayashi K, *et al*: Gefitinib or chemotherapy for non-small-cell lung cancer with mutated EGFR. N Engl J Med 362: 2380-2388, 2010.
9. Okamoto I, Yoshioka H, Morita S, *et al*: Phase III trial comparing oral S-1 plus carboplatin with paclitaxel plus carboplatin in chemotherapy-naïve patients with advanced non-small-cell lung cancer: results of a west Japan oncology group study. J Clin Oncol 28: 5240-5246, 2010.
10. Hanna N, Shepherd FA, Fossella FV, *et al*: Randomized phase III trial of pemetrexed versus docetaxel in patients with non-small-cell lung cancer previously treated with chemotherapy. J Clin Oncol 22: 1589-1597, 2004.
11. Pujol JL, Barlesi F and Daurès JP: Should chemotherapy combinations for advanced non-small cell lung cancer be platinum-based? A meta-analysis of phase III randomized trials. Lung Cancer 51: 335-345, 2006.
12. Gridelli C: The ELVIS trial: a phase III study of single-agent vinorelbine as first-line treatment in elderly patients with advanced non-small cell lung cancer. Elderly Lung Cancer Vinorelbine Italian Study. Oncologist 6 (Suppl 1): S4-S7, 2001.
13. Butts CA, Ding K, Seymour L, *et al*: Randomized phase III trial of vinorelbine plus cisplatin compared with observation in completely resected stage IB and II non-small-cell lung cancer: updated survival analysis of JBR-10. J Clin Oncol 28: 29-34, 2010.
14. Dunant A, Pignon JP and Le Chevalier T: Adjuvant chemotherapy for non-small cell lung cancer: contribution of the International Adjuvant Lung Trial. Clin Cancer Res 11: 5017s-5021s, 2005.
15. Douillard JY, Rosell R, De Lena M, *et al*: Adjuvant vinorelbine plus cisplatin versus observation in patients with completely resected stage IB-IIIA non-small-cell lung cancer (Adjuvant Navelbine International Trialist Association [ANITA]): a randomised controlled trial. Lancet Oncol 7: 719-727, 2006.
16. Nakagawa M, Tanaka F, Tsubota N, Ohta M, Takao M and Wada H; West Japan Study Group for Lung Cancer Surgery: A randomized phase III trial of adjuvant chemotherapy with UFT for completely resected pathological stage I non-small-cell lung cancer: the West Japan Study Group for Lung Cancer Surgery (WJSG) - the 4th study. Ann Oncol 16: 75-80, 2005.
17. Kato H, Ichinose Y, Ohta M, *et al*: A randomized trial of adjuvant chemotherapy with uracil-tegafur for adenocarcinoma of the lung. N Engl J Med 350: 1713-1721, 2004.
18. Matsumoto S, Igishi T, Hashimoto K, *et al*: Schedule-dependent synergism of vinorelbine and 5-fluorouracil/UFT against non-small cell lung cancer. Int J Oncol 25: 1311-1318, 2004.
19. Igishi T, Shigeoka Y, Yasuda K, *et al*: UFT plus vinorelbine in advanced non-small cell lung cancer: a phase I and an elderly patient-directed phase II study. J Thorac Oncol 4: 376-382, 2009.
20. Kodani M, Kinoshita N, Ueda Y, Suyama H, Sumikawa T, Makino H, Kurai J, Matsumoto S, Igishi T and Shimizu E: Phase II study of S-1 and vinorelbine in patients with advanced non-small cell lung cancer. Eur J Cancer 47 (Suppl 1): S620, 2011.
21. Mok TS, Wu YL, Thongprasert S, *et al*: Gefitinib or carboplatin-paclitaxel in pulmonary adenocarcinoma. N Engl J Med 361: 947-957, 2009.
22. Eisenhauer EA, Therasse P, Bogaerts J, *et al*: New response evaluation criteria in solid tumours: revised RECIST guideline (version 1.1). Eur J Cancer 45: 228-247, 2009.
23. Takata M, Chikumi H, Miyake N, *et al*: Lack of AKT activation in lung cancer cells with EGFR mutation is a novel marker of cetuximab sensitivity. Cancer Biol Ther 13: 369-378, 2012.
24. Das AK, Chen BP, Story MD, Sato M, Minna JD, Chen DJ and Nirodi CS: Somatic mutations in the tyrosine kinase domain of epidermal growth factor receptor (EGFR) abrogate EGFR-mediated radioprotection in non-small cell lung carcinoma. Cancer Res 67: 5267-5274, 2007.
25. Chou TC and Talalay P: Quantitative analysis of dose-effect relationships: the combined effects of multiple drugs or enzyme inhibitors. Adv Enzyme Regul 22: 27-55, 1984.
26. Khayat D, Rixe O, Brunet R, *et al*: Pharmacokinetic linearity of i.v. vinorelbine from an intra-patient dose escalation study design. Cancer Chemother Pharmacol 54: 193-205, 2004.
27. Dickgreber NJ, Fink TH, Latz JE, Hossain AM, Musib LC and Thomas M: Phase I and pharmacokinetic study of pemetrexed plus cisplatin in chemonaive patients with locally advanced or metastatic malignant pleural mesothelioma or non-small cell lung cancer. Clin Cancer Res 15: 382-389, 2009.
28. Hirata K, Horikoshi N, Aiba K, *et al*: Pharmacokinetic study of S-1, a novel oral fluorouracil antitumor drug. Clin Cancer Res 5: 2000-2005, 1999.
29. Muggia FM, Wu X, Spicer D, *et al*: Phase I and pharmacokinetic study of oral UFT, a combination of the 5-fluorouracil prodrug tegafur and uracil. Clin Cancer Res 2: 1461-1467, 1996.
30. Wu X, Sooman L, Lennartsson J, Bergström S, Bergqvist M, Gullbo J and Ekman S: Microtubule inhibition causes epidermal growth factor receptor inactivation in oesophageal cancer cells. Int J Oncol 42: 297-304, 2013.
31. Okabe T, Okamoto I, Tsukioka S, *et al*: Synergistic antitumor effect of S-1 and the epidermal growth factor receptor inhibitor gefitinib in non-small cell lung cancer cell lines: role of gefitinib-induced down-regulation of thymidylate synthase. Mol Cancer Ther 7: 599-606, 2008.
32. Wada Y, Yoshida K, Suzuki T, *et al*: Synergistic effects of docetaxel and S-1 by modulating the expression of metabolic enzymes of 5-fluorouracil in human gastric cancer cell lines. Int J Cancer 119: 783-791, 2006.

33. Hanada N, Lo HW, Day CP, Pan Y, Nakajima Y and Hung MC: Co-regulation of B-Myb expression by E2F1 and EGF receptor. Mol Carcinog 45: 10-17, 2006.
34. Ginsberg D: EGFR signaling inhibits E2F1-induced apoptosis in vivo: implications for cancer therapy. Sci STKE 2007: pe4, 2007.
35. Lee KH, Han SW, Hwang PG, *et al*: Epidermal growth factor receptor mutations and response to chemotherapy in patients with non-small-cell lung cancer. Jpn J Clin Oncol 36: 344-350, 2006.
36. Takano T, Fukui T, Ohe Y, *et al*: EGFR mutations predict survival benefit from gefitinib in patients with advanced lung adenocarcinoma: a historical comparison of patients treated before and after gefitinib approval in Japan. J Clin Oncol 26: 5589-5595, 2008.

PLOS ONE

Influence of Asian Dust Particles on Immune Adjuvant Effects and Airway Inflammation in Asthma Model Mice

Jun Kurai[1]*, Masanari Watanabe[1], Katsuyuki Tomita[2], Hiroyuki Sano Akira Yamasaki[3], Eiji Shimizu[1]

1 Department of Respiratory Medicine and Rheumatology, Tottori University Faculty of Medicine, Yonago, Tottori, Japan, **2** Department of Respiratory Medicine, Yonago Medical Center, Yonago, Tottori, Japan, **3** Department of Respiratory Medicine and Allergology, Kinki University Faculty of Medicine, Osaka-Sayama, Osaka, Japan

Abstract

Objective: An Asian dust storm (ADS) contains airborne particles that affect conditions such as asthma, but the mechanism of exacerbation is unclear. The objective of this study was to compare immune adjuvant effects and airway inflammation induced by airborne particles collected on ADS days and the original ADS soil (CJ-1 soil) in asthma model mice.

Methods: Airborne particles were collected on ADS days in western Japan. NC/Nga mice were co-sensitized by intranasal instillation with ADS airborne particles and/or Dermatophagoides farinae (Df), and with CJ-1 soil and/or Df for 5 consecutive days. Df-sensitized mice were stimulated with Df challenge intranasally at 7 days after the last Df sensitization. At 24 hours after challenge, serum allergen specific antibody, differential leukocyte count and inflammatory cytokines in bronchoalveolar lavage fluid (BALF) were measured, and airway inflammation was examined histopathologically.

Results: Co-sensitization with ADS airborne particles and Df increased the neutrophil and eosinophil counts in BALF. Augmentation of airway inflammation was also observed in peribronchiolar and perivascular lung areas. Df-specific serum IgE was significantly elevated by ADS airborne particles, but not by CJ-1 soil. Levels of interleukin (IL)-5, IL-13, IL-6, and macrophage inflammatory protein-2 were higher in BALF in mice treated with ADS airborne particles.

Conclusion: These results suggest that substances attached to ADS airborne particles that are not in the original ADS soil may play important roles in immune adjuvant effects and airway inflammation.

Citation: Kurai J, Watanabe M, Tomita K, Yamasaki HSA, Shimizu E (2014) Influence of Asian Dust Particles on Immune Adjuvant Effects and Airway Inflammation in Asthma Model Mice. PLoS ONE 9(11): e111831. doi:10.1371/journal.pone.0111831

Editor: Qinghua Sun, The Ohio State University, United States of America

Received May 21, 2014; **Accepted** October 7, 2014; **Published** November 11, 2014

Data Availability: The authors confirm that all data underlying the findings are fully available without restriction. All relevant data are within the paper.

Funding: This research was supported by the Environment Research and Technology Development Fund (5C-1154) of the Japanese Ministry of the Environment. The funders had no role in study design, data collection and analysis, decision to publish, or preparation of the manuscript.

Competing Interests: The authors have declared that no competing interests exist.

* Email: kurajun@med.tottori-u.ac.jp

Introduction

Many studies have shown that exposure to particulate matter is associated with respiratory and cardiovascular morbidity or mortality [1] [2]. Asian dust storms (ADSs) originating from deserts in Mongolia, Northern China, and Kazakhstan often disperse dust over East Asia from spring until late autumn [3] [4] and ADS airborne particles increase the atmospheric particulate matter. The original ADS soil is transported over a long distance and becomes attached to chemical species such as sulfate (SO_4^{2-}) and nitrate (NO^{3-}), and to microbial agents [5,6]. Therefore, ADS airborne particles have a wide variety of substances on their surface.

We have shown that ADS exposure can aggravate upper and lower tract respiratory symptoms and pulmonary dysfunction in adult patients with asthma [7] [8] [9]. Other studies have also found an association of an ADS with an increased risk of hospitalization in children with asthma [10] [11] [12]. These studies suggest that an ADS can exacerbate asthma, but the underlying mechanism remains unclear.

ADS airborne particles increase airway inflammation and have immune adjuvant effects in ovalbumin (OVA)-induced asthma model mice [13] [14] [15]. However, these studies used Asian sand dust after heat treatment at 360°C for 30 min to inactivate certain substances (microbiological material) attached on particles. Our previous study showed that ADS airborne particles induced production of IL-8 in THP-G8 cells, but this effect did not occur with the original ADS soil. Thus, substances attached to ADS airborne particles may provoke exacerbation of asthma. However, the OVA-induced asthma mouse model uses aluminum as an adjuvant, but aluminum is an important constituent of Asian sand dust [13]. The innovative asthma mouse model developed by Shibamori et al. shows allergic asthma-like reactions after intranasal sensitization by Dermatophagoides farinae (Df) [16]. Thus, these mice may be more useful than the OVA-induced model because the Df-induced asthma model does not require an adjuvant such as aluminum.

In this study, we explored the differences in immune adjuvant effects and airway inflammation between ADS airborne particles and original ADS soil, with the goal of investigating the mechanism of exacerbation of asthma caused by an ADS. The study was performed in Df-induced asthma model mice and

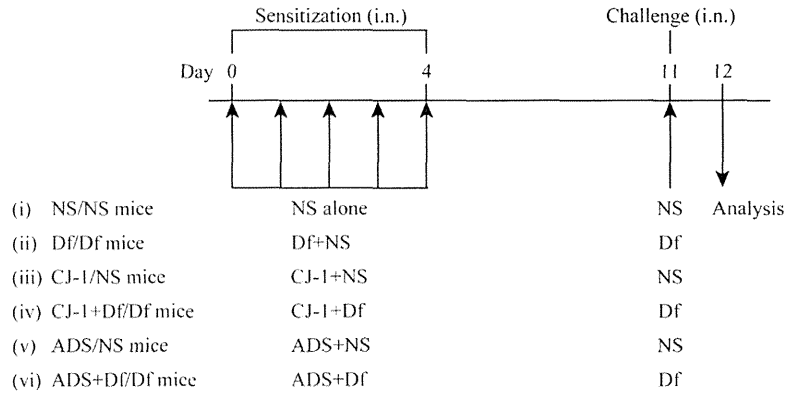

Figure 1. Experimental protocol. NC/Nga mice were given intranasal (i.n.) applications of a mixture (ADS airborne particles and/or Df, or CJ-1 soil and/or Df) as sensitization for 5 consecutive days (days 0–4). At 7 days after the last allergen sensitization, mice were challenged by allergen, followed by collection of BALF, lung tissue, and serum. Mice were divided into 6 groups: NS/NS, Df/Df, CJ-1/NS, CJ-1+Df/Df, ADS/NS, and ADS+Df/Df.
doi:10.1371/journal.pone.0111831.g001

without heating of the particles to avoid degradation of attached substances.

Materials and Methods

Animals

Specific pathogen-free 7-week-old male NC/Nga mice were purchased from Japan SLC Inc. (Hamamatsu, Japan) and acclimatized for 7 days before the start of the study. Animals were kept in a storage room at a constant temperature of 22°C and illumination with 12-hour light/dark cycles. Animals were fed standard animal chow daily and had access to drinking water ad libitum. The experimental protocols were approved by the Institutional Animal Care and Use Committee, Faculty of Medicine, Tottori University (protocol number 12-Y-55).

Preparation of ADS airborne particles and original ADS soil

CJ-1 soil from the China Loess Plateau, the original ADS soil in the Tengger Desert and Huining (Gansu Province), was obtained from the National Research Center for Environmental Analysis and Measurement (Ibaraki, Japan) in 2002. Airborne particles were collected in Tottori on ADS days from March 8 to March 11 in 2013 using a high-volume air sampler (HV-1000R; Shibata Co., Tokyo, Japan) which was fixed on the rooftop of a building. ADS airborne particles were separated according to their aerodynamic diameters into 5 filters (<1.1, 1.1–2.0, 2.0–3.3, 3.3–7.0, >7.0 μm) and each filter was dried in a desiccator before and after sampling to be weighted. In this study, we used ADS airborne particles whose size was 3.3–7.0 μm. CJ-1 soil and ADS airborne particles were sterilized at 121°C for 30 min in an autoclave (Tomy SX-300; Tomy Co., Tokyo, Japan) and stored in a freezer at −20 C° to prevent growth of bacteria and fungi. For administration to mice, CJ-1 soil and ADS airborne particles were diluted with normal saline (NS).

Experimental protocol

NC/Nga mice were sensitized to Df (Greer Laboratories Inc., Lenoir, NC, USA) as described elsewhere [16]. After a 7-day acclimatization period, mice were divided randomly into six groups (n = 8 per group). For sensitization, mice anesthetized by isoflurane inhalation were intranasally instilled with Df crude extract (50 μg) diluted with 25 μl of NS for 5 consecutive days (days 0–4). Df-sensitized mice were challenged intranasally with Df at 7 days after the last Df sensitization (day 11) and sacrificed 24 h after the Df challenge. In the control group, NS was administered instead of Df sensitization.

To observe immune adjuvant effects and airway inflammation induced by CJ-1 soil or ADS airborne particles (0.1 mg/25 μl of NS respectively), mice were co-sensitized by intranasal instillation of ADS airborne particles and/or Df, or CJ-1 soil and/or Df for 5 consecutive days (days 0–4) (Figure 1). The six groups were (i) NS/NS mice: sensitized with NS and challenged by NS; (ii) Df/Df mice: sensitized with Df and challenged by Df; (iii) CJ-1/NS mice: sensitized with CJ-1 soil and challenged by NS; (iv) CJ-1+Df/Df mice: co-sensitized with Df and CJ-1 soil and challenged by Df; (v) ADS/NS mice: sensitized with ADS airborne particles and challenged by NS; and (vi) ADS+Df/Df mice: co-sensitized with Df and ADS airborne particles and challenged by Df.

BALF procedure

After the mice were anesthetized with isoflurane, tracheas were cannulated. BALF was subsequently obtained with instillation of 1.0 ml NS into the lungs, along with gentle handling to maximize BALF recovery. BALF from each mouse was centrifuged at 300×g for 5 min at 4°C. The cell pellet was used for cell count and the supernatant was used for cytokine analysis. Total cells diluted in Turk's fluid were counted using a hemocytometer. The differential leukocyte count was obtained by microscopic evaluation and quantitative analysis of methanol-fixed cytospin preparations stained with Diff Quick (Fisher Scientific, Pittsburgh, PA, USA).

Histological examination

Mice were euthanized by injection of pentobarbital. Lungs were inflation-fixed at 25 cm of water pressure with 10% formalin for 5 min and immersed in the same fixative. Tissues were fixed for 24 h at 4°C and processed using standard methods for paraffin-embedded blocks. Fixed lung tissues were embedded in paraffin and each section was stained with hematoxylin-eosin (H&E) and periodic acid-Schiff/Alcian blue (PAS-AB).

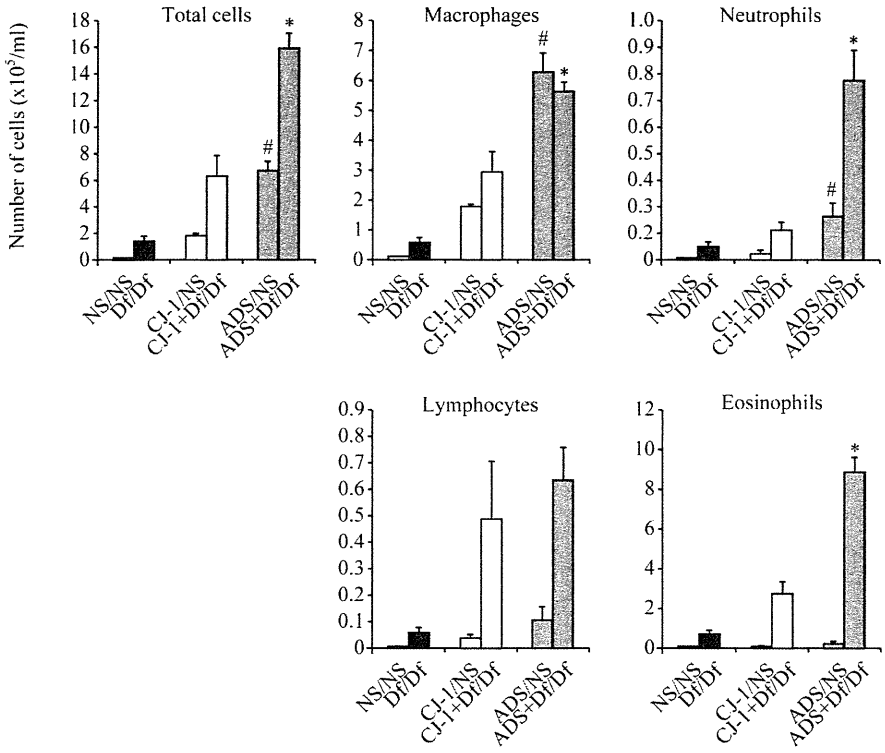

Figure 2. Total and differential leukocyte counts in BALF. The cell count in BALF was obtained from 24 h after allergen challenge on day 11. The differential leukocyte count was identified as eosinophils, macrophages, neutrophils, and lymphocytes. Total cell counts in ADS+Df/Df mice were increased significantly compared to CJ-1+Df/Df mice. Data are expressed as mean ±SD of 8 mice per group. *$p<0.05$ vs. CJ-1+Df/Df group, # $p<0.05$ vs. CJ-1/NS group.
doi:10.1371/journal.pone.0111831.g002

Enzyme-linked immunosorbent assay for serum total and Df-specific immunoglobulin

Total IgE and total IgG2a levels were measured with OptEIA Mouse kits (BD Pharmingen, San Diego, CA, USA). Df-specific IgE and Df-specific IgG2a levels were detected as previously described [17]. Briefly, 96-well plates were coated with a 50 μg/ml solution of Df and incubated overnight at 4°C. The content of each well was removed and the plate was washed with wash buffer (BD Pharmingen). Serum dilutions were 1/4 and 1/3000 for measuring Df-specific IgE and Df-specific IgG2a, respectively. The diluted serum was added to each well and incubated for 2 h at room temperature. Streptavidin-horseradish peroxidase conjugate (BD Pharmingen) was added to each well and incubated for 30 min at room temperature. The plate was developed with tetramethylbenzidine (100 μl/well) in the dark at room temperature for 30 min. The optical density (450 nm) was read with Sunrise, a microplate calibrated reader (Tecan Group, Japan), running the program XFluor4 (Tecan Group).

Cytokine and chemokine levels in BALF

Interferon (IFN)-γ, interleukin (IL)-13, IL-5, IL-6, keratinocyte-derived chemokine (KC/CXCL1), macrophage inflammatory protein (MIP)-2 (KC/CXCL1 and MIP-2/CXCL2 are murine homologues of human IL-8), thymus and activation-regulated chemokine (TARC/CCL17), and interferon gamma-induced protein (IP)-10/CXCL10 levels were measured by sandwich ELISA (R&D Systems Europe, Abingdon, UK). BALF dilutions were 1/5 for IL-13, IL-5, IL-6, KC/CXCL1, MIP-2/CXCL2, TARC/CCL17, and IP-10/CXCL10. BALF was undiluted for IFN-γ.

Statistical analysis

Data are expressed as mean and standard deviation (SD). Comparisons between groups were made by one-way ANOVA. Calculations were performed with GraphPadPrism ver. 5.02 (GraphPad Software, San Diego, CA, USA). $P<0.05$ was considered to be significant.

Results

Co-sensitization with ADS airborne particles and Df augments airway inflammation

Df/Df mice had a significant increase in total cell count in BALF compared to control NS/NS mice ($p<0.05$). In mice co-sensitized with CJ-1 soil and Df (CJ-1+Df/Df mice), the total cell count in BALF showed a significant 4.6-fold increase compared to Df/Df mice due to elevation of macrophages, lymphocytes and eosinophils (Figure 2). Mice co-sensitized with ADS airborne particles and Df (ADS+Df/Df mice) had greater enhancement of airway inflammation compared to CJ-1+Df/Df mice, and the total cell count was significantly increased by 2.5-fold in ADS+Df/Df mice (Figure 2). The increased cell count was consistent across macrophages, eosinophils and neutrophils, with significant elevations of 1.9-, 3.3-, and 6.2-fold, respectively, in ADS+Df/Df mice compared to CJ-1+Df/Df mice (Figure 2). The increase of

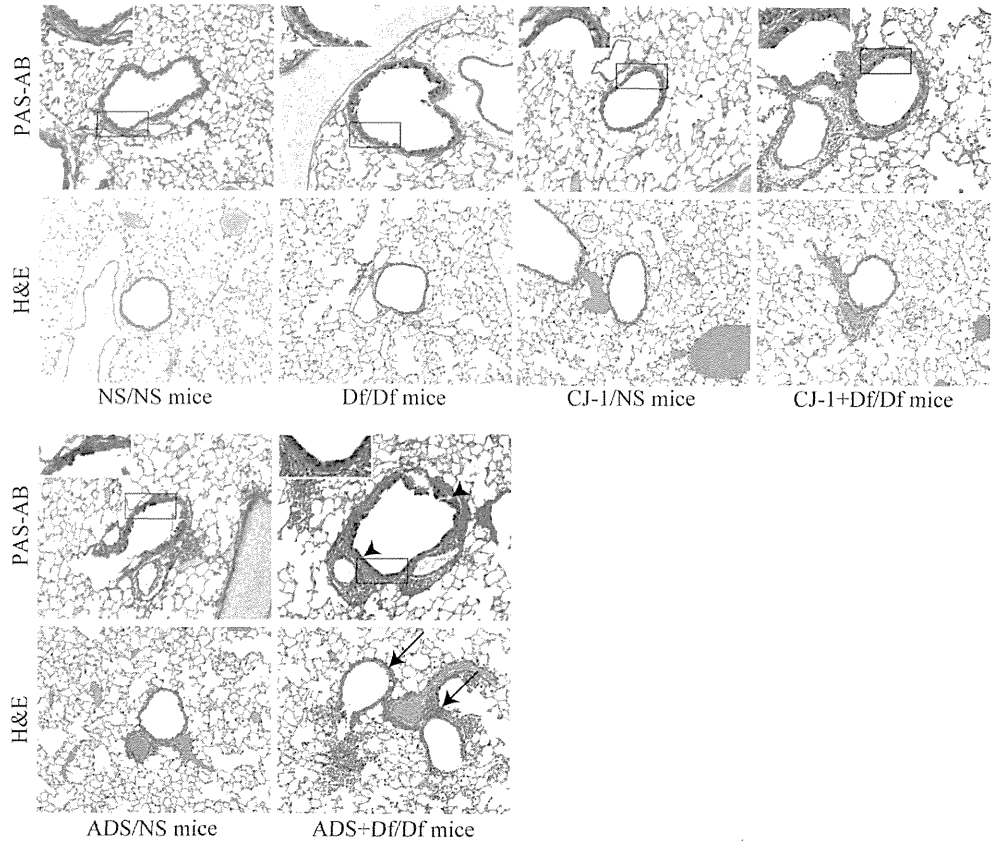

Figure 3. Effects of CJ-1 soil and ADS airborne particles on histopathological changes in lung. Light photomicrographs of representative lung sections stained with hematoxylin-eosin (magnification ×200) and periodic acid-Schiff/Alcian blue (magnification ×200). Representative light photomicrographs of NS/NS mice, Df/Df mice, CJ-1/NS mice, CJ-1+Df/Df mice, ADS/NS mice and ADS+Df/Df mice. Arrows show peribronchiolar and perivascular mixed inflammatory cell infiltration in ADS+Df/Df mice. Inset figure is higher magnification of the boxed area (magnification ×400). Arrow heads indicate the accumulation of mucus in the airway epithelial cells in ADS+Df/Df mice.
doi:10.1371/journal.pone.0111831.g003

neutrophils was most noticeable in the differential leukocyte count. There was no significant increase in lymphocytes.

Effects of ADS airborne particles on histopathological changes in lung

To determine the histopathological effects of co-sensitization with ADS airborne particles and Df on the airway, lung specimens were evaluated by staining with H&E and PAS-AB. CJ-1+Df/Df and ADS+Df/Df mice had greater peribronchiolar and perivascular inflammatory cell infiltration than CJ-1/NS and NS/AD mice, respectively. Greater airway inflammation was also apparent in ADS+Df/Df mice compared with CJ-1+Df/Df mice (Figure 3, H&E staining). Df/Df mice showed relatively weaker inflammatory responses than ADS+Df/Df and CJ-1+Df/Df mice. These histopathological findings were consistent with the BALF analysis. Furthermore, there was a markedly greater mucus cell metaplasia with increased amounts of PAS-AB-stained mucosubstances on the surface epithelium in ADS+Df/Df mice compared with CJ-1+Df/Df mice (Figure 3, PAS-AB staining).

Co-sensitization with ADS airborne particles and Df potentiates immune adjuvant effects

To examine the immune adjuvant effects of CJ-1 soil and ADS airborne particles in Df-sensitized mice, serum immunoglobulin levels were evaluated on day 12. ADS+Df/Df mice had significantly increased total IgE and total IgG2a (1.9- and 1.6-fold, respectively, as immunoglobulin concentrations, $p<0.05$) and Df-specific IgE ($p<0.05$) compared to CJ-1+Df/Df mice (Figure 4). In contrast, co-sensitization with CJ-1 soil and Df (CJ-1+Df/Df mice) had no effect on total IgE, total IgG2a, Df-specific IgE, and Df-specific IgG2a levels (Figure 4). These data indicate that ADS airborne particles recruit inflammatory cells into lung tissues and potentiate immune adjuvant effects, whereas CJ-1 soil does not have these effects.

Co-sensitization with ADS airborne particles and Df induces production of Th2 and inflammatory cytokines

To investigate the mechanisms through which ADS airborne particles cause an allergic airway response in Df-induced asthma model mice, cytokine levels in BALF were measured. In parallel with the inflammatory cell recruitment in BALF, ADS airborne particles induced production of several important cytokines for

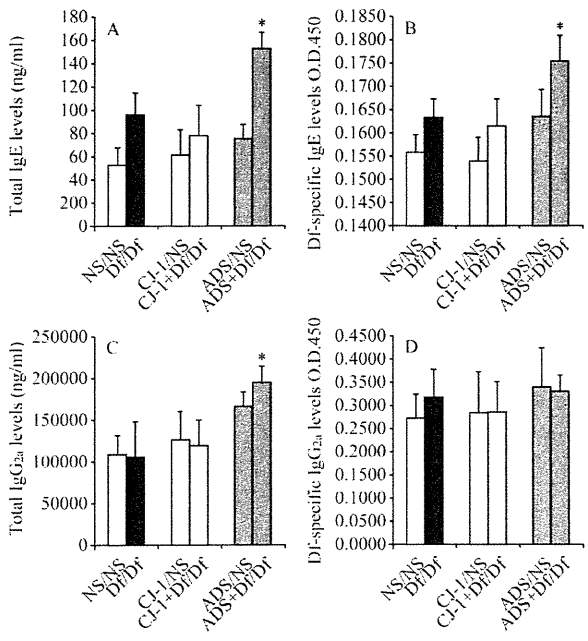

Figure 4. Total IgE, total IgG2a, Df-specific IgE, and Df-specific IgG2a levels in serum. Serum total IgE (A) and total IgG2a (C) were measured by ELISA and are shown as serum concentrations. Df-specific IgE (B) and Df-specific IgG2a (D) were measured based on optical density. Results are expressed as mean ±SD of 6 mice per group. *$p<0.05$ vs. CJ-1+Df/Df group.
doi:10.1371/journal.pone.0111831.g004

asthma. BALF from ADS+Df/Df mice had higher levels of Th2 cytokines (IL-5, IL-13); inflammatory cytokines (IL-6, MIP-2/CXCL2), except for KC/CXCL1, a neutrophil activation chemokine; and a Th2 chemokine (TARC/CCL17), compared to CJ-1+Df/Df and Df/Df mice (Figure 5). In contrast to ADS+Df/Df mice, CJ-1+Df/Df mice did not have significant increases in cytokine and chemokine levels compared to control Df/Df mice. A Th1 cytokine (IFN-γ) and a Th1 chemokine (IP-10/CXCL10) showed no increase after administration of CJ-1 soil or ADS airborne particles.

Discussion

This study shows that airborne particles collected on ADS days have significantly different effects as an immune adjuvant and on airway inflammation compared to original ADS soil. The ADS airborne particles significantly increased the number of neutrophils and eosinophils in BALF, and significantly augmented airway inflammation with mucus hypersecretion compared to the original ADS soil. The particles also induced significant elevation of serum total IgE, total IgG2a, and Df-specific IgE, but the original ADS soil did not do so. ADS airborne particles also increased production of inflammatory cytokines (IL-6 and MIP-2/CXCL2) and Th2 cytokines (IL-5 and IL-13). These results suggest that substances attached to ADS airborne particles augment airway inflammation and increase immune adjuvant effects.

Air pollutants augment human airway inflammation through effects on IL-8 and IL-6 [18] [19] [9], and IL-8 and IL-6 have important roles in neutrophilic airway inflammation in patients with asthma [20] [21] [22]. There were significant increases in MIP-2/CXCL2 (a murine homologue of IL-8) and IL-6 and in the neutrophil count in BALF of ADS+Df/Df mice compared to CJ-1+Df/Df mice. This implies that ADS airborne particles have a stronger effect than CJ-1 soil in inducing neutrophilic airway inflammation via MIP-2/CXCL2 and IL-6 elevation. Honda et al. showed that IL-8 and IL-6 increase in a dose-dependent manner after exposure of airway epithelial cells to ADS airborne particles *in vitro* [23], and also found that these particles did not induce IL-8 and IL-6 after cauterization to eliminate attached substances.

These results suggest that the different effects of ADS airborne particles and original ADS soil may depend on substances such as chemicals and microorganisms attached to the particles. It is unclear which of these substances has most toxicity in human health. Inhaled LPS is associated with neutrophilic airway inflammation in healthy subjects and patients with asthma [24] [25]; and He et al. found that ADS airborne particles have LPS on their surface [26], but that the original ADS soil does not contain LPS. Thus, LPS on the particles may have an important role in inducing neutrophilic airway inflammation via MIP-2/CXCL2 and IL-6 elevation.

Co-sensitization with ADS airborne particles and Df increased the number of eosinophils and elevated IL-5 and IL-13 in BALF. The increase in neutrophils in BALF was also greater than that of eosinophils in ADS+Df/Df mice. Thus, exacerbation of asthma by an ADS may be more closely linked to neutrophilic airway inflammation. ADS airborne particles also increased serum total IgE, total IgG2a and Df-specific IgE, indicating that these particles have immune adjuvant effects. In contrast, CJ-1 soil did not increase Th2 cytokines (IL-5, IL-13) or immunoglobulins, which suggests that substances on ADS airborne particles contribute to production of Th2 cytokines, total IgE, total IgG2a and Df-specific IgE.

OVA is often used as an allergen in asthma model mice, but OVA is not the major allergen in asthma. OVA-induced model mice are also sensitized with intraperitoneal injection of aluminum as an adjuvant, but aluminum is an important component of Asian sand dust [13]. This suggests that it may be difficult to assess the adverse effect of ADS airborne particles in OVA-induced model mice. Previous study also showed that even an amorphous silica, which is a major component of Asian sand dust, may also potentiate the immune adjuvant effect by itself [27], though we could not detect it in our study. We cannot exclude an immune adjuvant effect of aluminum in ADS airborne particles, but administration of these particles was performed by intranasal instillation, rather than intraperitoneal injection (as used in OVA-induced model mice). Thus, we believe that Df-induced NC/Nga asthma model mice are useful for accurate evaluation of the influence of ADS airborne particles because this mouse model does not require an adjuvant and is challenged with an allergen that closely resembles that in human asthma.

There are several limitations in this study. First, we did not analyze the composition of the ADS airborne particles in detail. Thus, we cannot identify the attached substances that increased immune adjuvant effects and airway inflammation. Second, we were unable to collect sufficient amounts of ADS airborne particles for use in the challenge, and this prevented investigation of the effects of the particles in this phase. Third, we did not evaluate airway hyperresponsiveness (AHR), though previous study shows significant increases in AHR after intranasal administration of Df in this asthma mice model [16]. Therefore, the present study could not show that airborne particles collected on ADS days may provoke exacerbation of asthma functionally. Finally, although use of NC/Nga mice strains combined with Df sensitization and challenge protocols is likely to be meaningful, human patients with

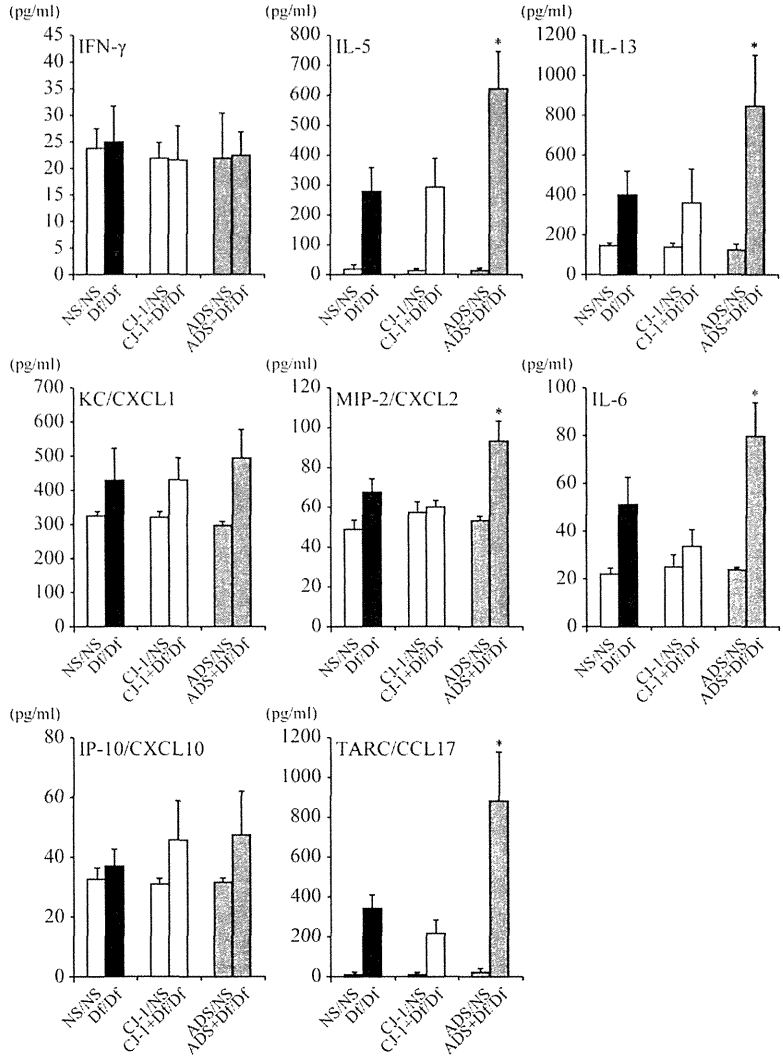

Figure 5. Cytokines and chemokines levels in BALF. BALF cytokine and chemokine expression profiles were analyzed by ELISA for IFN-γ, IL-5, IL-13, IP-10/CXCL10, TARC/CCL17, KC/CXCL1, MIP-2/CXCL2 and IL-6. Data for each group are expressed as mean ±SD of 6 mice per group. *$p<0.05$ vs. CJ-1+Df/Df groups.
doi:10.1371/journal.pone.0111831.g005

asthma are a heterogeneous population defined by unique interactions between genetic and environmental factors. Hence, exposure to ADS airborne particles may lead to different types of health damage in different individuals.

In summary, this is the first report to show that airborne particles collected on ADS days in western Japan, but not the original ADS soil, have immune adjuvant effects, augment airway inflammation via an increase of neutrophils and promote mucus hypersecretion. These results suggest that substances attached to ADS airborne particles play important roles in exacerbating asthma upon exposure to an ADS. Further studies are required to investigate the mechanisms how substances attached to ADS airborne particles augment airway inflammation, and which substances play more important role.

Author Contributions

Conceived and designed the experiments: JK MW KT HS AY ES. Performed the experiments: JK. Analyzed the data: JK. Wrote the paper: JK.

References

1. Dockery DW, Pope CA 3rd, Xu X, Spengler JD, Ware JH, et al. (1993) An association between air pollution and mortality in six U.S. cities. N Engl J Med 329: 1753–1759.

2. Ware JH, Thibodeau LA, Speizer FE, Colome S, Ferris BG Jr (1981) Assessment of the health effects of atmospheric sulfur oxides and particulate matter: evidence from observational studies. Environ Health Perspect 41: 255–276.

3. Duce RA, Unni CK, Ray BJ, Prospero JM, Merrill JT (1980) Long-range atmospheric transport of soil dust from Asia to the tropical north pacific: temporal variability. Science 209: 1522–1524.
4. Taylor DA (2002) Dust in the wind. Environ Health Perspect 110: A80–87.
5. Chen PS, Tsai FT, Lin CK, Yang CY, Chan CC, et al. (2010) Ambient influenza and avian influenza virus during dust storm days and background days. Environ Health Perspect 118: 1211–1216.
6. Maki T, Susuki S, Kobayashi F, Kakikawa M, Tobo Y, et al. (2010) Phylogenetic analysis of atmospheric halotolerant bacterial communities at high altitude in an Asian dust (KOSA) arrival region, Suzu City. Sci Total Environ 408: 4536–4562.
7. Watanabe M, Igishi T, Burioka N, Yamasaki A, Kurai J, et al. (2011) Pollen augments the influence of desert dust on symptoms of adult asthma patients. Allergol Int 60: 517–524.
8. Watanabe M, Yamasaki A, Burioka N, Kurai J, Yoneda K, et al. (2011) Correlation between Asian dust storms and worsening asthma in Western Japan. Allergol Int 60: 267–275.
9. Watanabe M, Kurai J, Tomita K, Sano H, Abe S, et al. (2014) Effects on asthma and induction of interleukin-8 caused by Asian dust particles collected in western Japan. J Asthma.
10. Kanatani KT, Ito I, Al-Delaimy WK, Adachi Y, Mathews WC, et al. (2010) Desert dust exposure is associated with increased risk of asthma hospitalization in children. Am J Respir Crit Care Med 182: 1475–1481.
11. Ueda K, Nitta H, Odajima H (2010) The effects of weather, air pollutants, and Asian dust on hospitalization for asthma in Fukuoka. Environ Health Prev Med 15: 350–357.
12. Yoo Y, Choung JT, Yu J, Kim do K, Koh YY (2008) Acute effects of Asian dust events on respiratory symptoms and peak expiratory flow in children with mild asthma. J Korean Med Sci 23: 66–71.
13. Ichinose T, Yoshida S, Sadakane K, Takano H, Yanagisawa R, et al. (2008) Effects of asian sand dust, Arizona sand dust, amorphous silica and aluminum oxide on allergic inflammation in the murine lung. Inhal Toxicol 20: 685–694.
14. Ichinose T, Yoshida S, Hiyoshi K, Sadakane K, Takano H, et al. (2008) The effects of microbial materials adhered to Asian sand dust on allergic lung inflammation. Arch Environ Contam Toxicol 55: 348–357.
15. He M, Ichinose T, Yoshida S, Nishikawa M, Mori I, et al. (2010) Airborne Asian sand dust enhances murine lung eosinophilia. Inhal Toxicol 22: 1012–1025.
16. Shibamori M, Ogino K, Kambayashi Y, Ishiyama H (2006) Intranasal mite allergen induces allergic asthma-like responses in NC/Nga mice. Life Sci 78: 987–994.
17. Fukuyama T, Tajima Y, Hayashi K, Ueda H, Kosaka T (2011) Prior or coinstantaneous oral exposure to environmental immunosuppressive agents aggravates mite allergen-induced atopic dermatitis-like immunoreaction in NC/Nga mice. Toxicology 289: 132–140.
18. Bellido-Casado J, Plaza V, Perpina M, Picado C, Bardagi S, et al. (2010) [Inflammatory response of rapid onset asthma exacerbation]. Arch Bronconeumol 46: 587–593.
19. Wittkopp S, Staimer N, Tjoa T, Gillen D, Daher N, et al. (2013) Mitochondrial genetic background modifies the relationship between traffic-related air pollution exposure and systemic biomarkers of inflammation. PLoS One 8: e64444.
20. Wood LG, Baines KJ, Fu J, Scott HA, Gibson PG (2012) The neutrophilic inflammatory phenotype is associated with systemic inflammation in asthma. Chest 142: 86–93.
21. Pepe C, Foley S, Shannon J, Lemiere C, Olivenstein R, et al. (2005) Differences in airway remodeling between subjects with severe and moderate asthma. J Allergy Clin Immunol 116: 544–549.
22. Shannon J, Ernst P, Yamauchi Y, Olivenstein R, Lemiere C, et al. (2008) Differences in airway cytokine profile in severe asthma compared to moderate asthma. Chest 133: 420–426.
23. Honda A, Matsuda Y, Murayama R, Tsuji K, Nishikawa M, et al. (2013) Effects of Asian sand dust particles on the respiratory and immune system. J Appl Toxicol.
24. Alexis NE, Peden DB (2006) Inflammatory response of the airway to inhaled endotoxin correlates with body mass index in atopic patients with asthma but not in normal volunteers. J Allergy Clin Immunol 117: 1185–1186.
25. Alexis N, Eldridge M, Reed W, Bromberg P, Peden DB (2001) CD14-dependent airway neutrophil response to inhaled LPS: role of atopy. J Allergy Clin Immunol 107: 31–35.
26. He M, Ichinose T, Song Y, Yoshida Y, Arashidani K, et al. (2013) Effects of two Asian sand dusts transported from the dust source regions of Inner Mongolia and northeast China on murine lung eosinophilia. Toxicol Appl Pharmacol 272: 647–655.
27. Mancino D, Ovary Z (1980) Adjuvant effects of amorphous silica and of aluminium hydroxide on IgE and IgG1 antibody production in different inbred mouse strains. Int Arch Allergy Appl Immunol 61: 253–258.

Environmental Research 134 (2014) 188–189

Contents lists available at ScienceDirect

Environmental Research

journal homepage: www.elsevier.com/locate/envres

Commentary

Definition of Asian dust particles

Masanari Watanabe*, Jun Kurai, Eiji Shimizu

Department of Respiratory Medicine and Rheumatology, Faculty of Medicine, Tottori University, 36-1 Nishimachi, Yonago 683-8504, Japan

ARTICLE INFO

Article history:
Received 28 May 2014
Received in revised form
9 July 2014
Accepted 20 July 2014
Available online 28 August 2014

To the Editor:

We write with regard to the interesting article by Mimura et al. (2014) showing that Asian dust acts as an adjuvant to promote allergic disease induced by inhaled allergens such as pollen and fungi. In a previous study, we showed that airborne particles collected on days of Asian dust storms (ADSs) in western Japan had significantly different effects on induction of secretion of interleukin (IL)-8, compared to the origin soil of the ADS (Watanabe et al., 2014). We proposed that this difference may be caused by substances such as chemicals, metals and microorganisms carried by the ADS, in agreement with the findings of Honda et al. (2014).

There is no absolute definition of an ADS day and this causes difficulty in comparison of studies. The Japan Meteorological Agency has observatories throughout Japan and defines an ADS day using a criterion of visibility < 10 km due to dust arising from the deserts of East Asia, as determined by meteorological satellites monitoring each area. Recently, the Japanese Ministry of the Environment has used Light Detection and Ranging (LIDAR) to define ADS days. LIDAR can be used to measure the level of mineral dust particles as airborne sand dust and non-mineral dust particles as air-pollution aerosols in real time (Sugimoto and Lee, 2006; Sugimoto et al., 2008). Other studies have defined ADS events as a daily (24-h) average of mineral dust particles $> 0.1\ km^{-1}$ (Kanatani et al., 2010) or $0.066\ km^{-1}$ (moderate ADS day) and $0.105\ km^{-1}$ (heavy ADS day) (Ueda et al., 2012). The definition of an ADS day is not stated by Mimura et al. In 2011, May 2nd and 3rd were identified as ADS days in Tokyo by the Japan Meteorological Agency (http://www.data.kishou.go.jp/obs-env/kosahp/kosa_table_2011.html). An ADS event, as defined above, was not detected anywhere Japan on 6 March 2011, the day on which it is stated that ADS airborne particles were collected in Mimura et al. The daily average levels of mineral dust particles and non-mineral dust particles in Tokyo based on LIDAR from 2 March to 31 May in 2011 are shown in Fig. 1. The daily average level of mineral dust particles on 6 March 2011 was $0.037\ km^{-1}$.

In Mimura et al., skin prick tests with untreated Asian dust, Asian dust extract, heat-sterilized Asian dust, silicon dioxide (SiO_2), and phosphate-buffered saline (PBS) were performed to evaluate sensitization to Asian dust in patients with rhinoconjunctivitis. Skin prick tests are recommended as the primary method for diagnosis of IgE-mediated allergies in most allergic diseases, but cannot be used to investigate sensitization effects. Crystalline silica can stimulate production of IgE and IgG_1 antibodies in BALB/c mice with a single 1 μg dose of ovalbumin

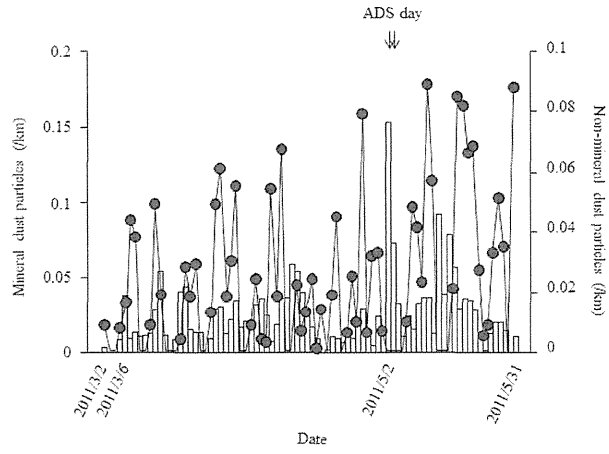

Fig. 1. Daily average levels of mineral dust particles (airborne sand dust particles) and non-mineral dust particles (air-pollution aerosols). The bar graph shows the level of mineral dust particles and the line graph represents that of non-mineral dust particles. Arrows indicate the ADS day by the Japan Meteorological Agency.

* Corresponding author. Fax: +81 859 38 6539.
E-mail address: watanabm@med.tottori-u.ac.jp (M. Watanabe).

http://dx.doi.org/10.1016/j.envres.2014.07.011
0013-9351/

(Mancino and Ovary, 1980). Certain low-molecular-weight agents, such as platinum salts, trimellitic anhydrate and other acidanhydrate, are also able to induce specific IgE, but they act as a hapten and combine with a body protein to form functional antigens (Mapp et al., 2005). In Mimura et al., both the allergic and atopic groups both had patients with positive responses to SiO_2 and sterilized Asian dust in skin prick tests. Does this suggest that silica has an antigen-specific IgE?

References

Honda, A., Matsuda, Y., Murayama, R., Tsuji, K., Nishikawa, M., Koike, E., Yoshida, S., Ichinose, T., Takano, H., 2014. Effects of Asian sand dust particles on the respiratory and immune system. J. Appl. Toxicol. 34, 250–257.

Kanatani, K.T., Ito, I., Al-Delaimy, W.K., Adachi, Y., Mathews, W.C., Ramsdell, J.W., 2010. Toyama Asian Desert Dust and Asthma Study TeamDesert-dust exposure is associated with increased risk of asthma hospitalization in children. Am. J. Respir. Crit. Care Med. 182, 1475–1481.

Mancino, D., Ovary, Z., 1980. Adjuvant effects of amorphous silica and of aluminium hydroxide on IgE and IgG1 antibody production in different inbred mouse strains. Int. Arch. Allergy Appl. Immunol. 61, 253–258.

Mapp, C.E., Boschetto, P., Maestrelli, P., Fabbri, L.M., 2005. Occupational asthma. Am. J. Respir. Crit. Care Med. 172, 280–305.

Mimura, T., Yamagami, S., Fujishima, H., Noma, H., Kamei, Y., Goto, M., Kondo, A., Matsubara, M., 2014. Sensitization to Asian dust and allergic rhinoconjunctivitis. Environ. Res. 132C, 220–225. http://dx.doi.org/10.1016/j.envres.2014.04.014.

Sugimoto, N., Lee, C.H., 2006. Characteristics of dust aerosols inferred from LIDAR depolarization measurements at two wavelengths. Appl. Opt. 45, 7468–7474.

Sugimoto, M., Matsui, I., Shimizu, A., Nishizawa, T., Hara, Y., Xie, C., Uno, I., Yumimoto, K., Wang, Z., Yoon, S-C., 2008. Lidar network observations of tropospheric aerosols. Proc. SPIE 2008, 7153. http://dx.doi.org/10.1117/12.806540.

Ueda, K., Shimizu, A., Nitta, H., Inoue, K., 2012. Long-range transported Asian dust and emergency ambulance dispatches. Inhal. Toxicol. 24, 858–867.

Watanabe, M., Kurai, J., Tomita, K., Sano, H., Abe, S., Saito, R., Minato, S., Igishi, T., Burioka, N., Sako, T., Yasuda, K., Mikami, M., Kurita, S., Tokuyasu, H., Ueda, Y., Konishi, T., Yamasaki, A., Aiba, S., Oshimura, M., Shimizu, E. 2014. Effects on asthma and induction of interleukin-8 caused by Asian dust particles collected in western Japan. J. Asthma (Epub ahead of print).

REVIEW

The molecular biology of lung cancer brain metastasis : an overview of current comprehensions and future perspectives

Masaki Hanibuchi[1], Sun-Jin Kim[2], Isaiah J. Fidler[2], and Yasuhiko Nishioka[1]

[1]*Department of Respiratory Medicine and Rheumatology, Institute of Health Biosciences, The University of Tokushima Graduate School, Tokushima, Japan,* [2]*Department of Cancer Biology, The University of Texas M. D. Anderson Cancer Center, Houston, USA*

Abstract : Brain metastases occur in 20-40% of patients with advanced malignancies and lung cancer is one of the most common causes of brain metastases. The occurrence of brain metastases is associated with poor prognosis and high morbidity in patients with advanced lung cancer, even after intensive multimodal therapy. Progress in treating brain metastases has been hampered by a lack of model systems, a lack of human tissue samples, and the exclusion of brain metastatic patients from many clinical trials. While the biology of brain metastasis is still poorly understood, it is encouraging to see more efforts are beginning to be directed toward the study of brain metastasis. During the multi-step process of metastasis, functional significance of gene expressions, changes in brain vasculature, abnormal secretion of soluble factors and activation of autocrine/paracrine signaling are considered to contribute to the brain metastasis development. A better understanding of the mechanism of this disease will help us to identify the appropriate therapeutic strategies, which leads to circumvent brain metastases. Recent findings on the biology of lung cancer brain metastases and translational leads identified by molecular studies are discussed in this review. J. Med. Invest. 61 : 241-253, August, 2014

Keywords **:** *brain metastasis, lung cancer, molecular biology*

I. INTRODUCTION

Brain metastases constitute the most frequent malignant disease in the central nervous system (CNS), outnumbering primary brain tumor cases 10-fold (1). Up to 20-40% of patients with adult systemic malignancies will develop brain metastases in the course of their disease (2). A variety of systemic malignancies can metastasize to the CNS, although the majority of the lesions come from lung cancer

Abbreviation used : CNS, central nervous system ; QOL, quality of life ; NSCLC, non-small cell lung cancer ; SCLC, small cell lung cancer ; WBRT, whole brain radiation therapy ; BBB, blood-brain barrier ; TJ, tight junction ; ECM, extracellular matrix ; ICAM, intercellular adhesion molecule ; VCAM, vascular-cell adhesion molecule ; PECAM, platelet-endothelial-cell adhesion molecule ; EMT, epithelial-mesenchymal transition ; VEGF, vascular endothelial growth factor ; PlGF, placental growth factor ; MMP, matrix metalloproteinase ; ADAM, a disintegrin and metalloprotease ; EGFR, epidermal growth factor receptor ; ALK, anaplastic lymphoma kinase ; ROCK, Rho kinase ; HGF, hepatocyte growth factor ; PI3K, phosphoinositide 3-kinase ; ET, endothelin ; miRNA, microRNA ; SNP, single nucleotide polymorphism ; TGF-β, transforming growth factor-β ; CEA, carcinoembronic antigen ; ProGRP, pro-gastrin-releasing peptide ; PCI, prophylactic cranial irradiation ; IL, interleukin ; TNF-α, tumor necrosis factor-α ; EGFR-TKI, epidermal growth factor receptor-tyrosine kinase inhibitor ; CSF, cerebrospinal fluid ; EML4, microtubule-associated protein-like 4

Received for publication May 27, 2014 ; accepted June 23, 2014.

Address correspondence and reprint requests to Yasuhiko Nishioka, Department of Respiratory Medicine and Rheumatology, Institute of Health Biosciences, the University of Tokushima Graduate School, 3-18-15 Kuramoto-cho Tokushima, 770-8503, Japan and Fax : +81-88-633-2134.

(40-50%) followed by breast cancer (20-30%), melanoma (5-10%), lymphoma, and various other primary sites like the gastrointestinal tract (4-6%) and prostate (3, 4). Brain metastasis represents a significant healthcare problem and has an adverse impact on patient morbidity and outcome (5). In addition, tumors in the CNS strongly affect patients' quality of life (QOL), impairing sensory and motor neural functions and inducing headache, nausea, vomiting, and seizures (6). While conventional treatment regimens provide marginal survival benefits (7), the prognosis for patients with brain metastases is dismal. With an increasing incidence (8), and a frequent occurrence in patients whose extracranial cancer has been controlled, brain metastasis is becoming a major limiting factor for cancer patients' QOL and survival.

Lung cancer, including non-small cell lung cancer (NSCLC) and small cell lung cancer (SCLC), is the leading cause of malignancy-related death worldwide. Lung cancer is the malignancy that most commonly gives rise to brain metastases. Approximately 10-25% of lung cancer patients have brain metastases at initial diagnosis and about 40-50% of them develop brain metastases during the course of disease (9). Treatment options are limited and standard of care is generally whole brain radiation therapy (WBRT) with corticosteroids to alleviate edema and overall survival is 3-6 months after diagnosis of CNS disease. Favorable prognostic factors that affect survival include Karnofsky's performance status, patient age (< 65 years), control of primary tumor, and absence of extracranial metastatic disease (10). To overcome lung cancer brain metastases, an understanding of the molecular biology of brain metastasis is crucial. The current review gives a broad overview about the accumulating recent knowledge of lung cancer brain metastasis and the latest developments in the field.

II. BIOLOGY OF BRAIN METASTASIS

Similar to the metastatic process in other organs, brain metastasis formation is a highly selective, multi-step process, involving complex interactions between tumor and host cells, which is clearly explained by the "seed-and-soil" hypothesis (11, 12).

The brain is considered as a "sanctuary" site for metastatic cancer cells because many of the therapeutic agents can not cross the blood-brain barrier (BBB) (13). The BBB is a network composed of both endothelial cells and supporting components that protects the CNS microenvironment. In contrast to the periphery, the endothelium of brain micro-vessels is characterized by continuous tight junctions (TJs), decreased pinocytosis activity, very low pinocytic activity, and overexpressed efflux pumps (14) (Figure 1). With the reinforcement of the surrounding extracellular matrix (ECM), basal membrane, pericytes, and the end-feet of astrocytes, the BBB effectively prevents the free exchange of substances between the blood and the interstitial fluid of the brain (15). Therefore, the brain forms a special challenge for tumor cells because of BBB and all other steps have to be successfully completed

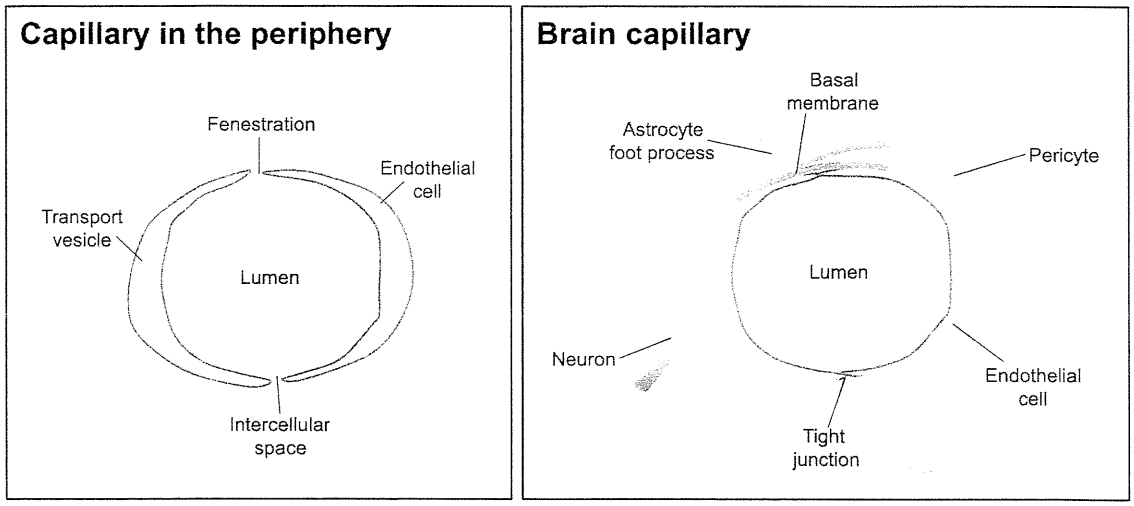

Figure 1. Schematic comparison of a brain capillary with a capillary in the periphery. Schematic structure of the blood-brain barrier. Cerebral endothelial cells, coming in contact with pericytes and astrocytes, form the morphological basis of the blood-brain barrier. Endothelial cells are interconnected by a continuous line of tight junctions (Cited from reference number 14 and revised).

for tumor cells to invade through BBB and survive.

When metastatic cancer cells enter the brain circulation, they might arrest in sites of slow flow within the capillary bed at vascular branch points. Then, interactions between cancer cells and brain endothelial cells or transendothelial migration are mediated by interaction of tumor cell-surface receptors and endothelial cell adhesion molecules (16). After overcoming the BBB, tumor cells are confronted with components of the local microenvironment including the extracellular matrix (ECM), resident brain parenchymal cells (astrocytes, microglia), and paracrine signaling molecules including cytokines and growth factors (16). Survival and successful tumor growth require adaption to and interaction with these factors. The brain also establishes an adequate blood supply via angiogenesis, angioectasia, vasculogenesis, vasculogenic mimicry, making brain metastases grow and proliferate better (17). During the above process, functional significance of gene expressions, changes in brain vasculature, abnormal secretion of soluble factors and activation of autocrine/paracrine signaling contribute to the brain metastasis development.

III. MOLECULAR PATHWAYS MEDIATING LUNG CANCER BRAIN METASTASIS

1. Gene expression analyses

In order to identify pathways specific to the development of brain metastasis and novel molecular targets/translational leads, several groups have undertaken gene expression studies in animal models and human tissue cohorts.

Kikuchi *et al.* compared gene expression of primary lung adenocarcinoma with brain metastases originating from these tumors. Of 23,040 genes tested, 244 showed a different expression level, including genes coding for plasma membrane proteins, cellular antigens and cytoskeletal proteins, which may modulate cell-cell interactions (18). Brain metastases of lung adenocarcinoma were evaluated in another study as well, by comparing the gene expression profile of metastatic brain tumors originating from lung adenocarcinoma with that of healthy lung. Zohrabian *et al.* have found 1,561 differently expressed genes by using cDNA microarray. The overexpression of genes associated with invasion and metastasis, adhesion, angiogenesis and cell migration was validated by real-time PCR (19).

In a cohort of primary tumors from lung cancer patients who developed brain metastases, Grinberg-Rashi *et al.* found the expression levels of three genes, CDH2, KIFC1, and FALZ, was highly predictive of brain metastases (20). N-cadherin, which is coded by CDH2 gene, is involved in multiple processes including inducing invasion, migration, promoting survival of cancer cells, regulating adhesion and neurite outgrowth (21). Clinically, N-cadherin overexpression has been shown to be associated with decreased survival in poorly differentiated SCLCs (22).

DCUN1D1, a squamous cell carcinoma-related oncogene, is associated with tumor progression and poor outcomes in NSCLC. Recently, the overexpression of DCUN1D1 has been found to be useful in identifying patients who are at higher risk for brain metastases. Yoo *et al.* showed that 14 of 16 DCUN1D1-positive NSCLC patients (87.5%) resulted in brain metastases (23).

However, as previously reported in other primary and metastatic clinical or experimental tumors (24-26), the genetic heterogeneity would limit the translation of the gene profiles into the clinical trials.

2. Cell surface molecules

1) Integrins

Integrins are a family of cell surface receptors that mediate cell adhesion and signal transduction. Integrins interact with ECM components such as collagen, laminin, and fibronectin and play crucial roles in cell migration. Integrins can also activate signaling cascades to mediate cell survival (27). The expression of integrin $\alpha3\beta1$ has been associated with lung cancer brain metastasis. Compared with their parental cell line and bone-metastasizing counterparts, tumor cells that preferably metastasize to the brain highly expressed $\alpha3\beta1$ integrin (28). Moreover, inhibiting $\alpha3\beta1$ integrin function decreased brain metastases formation in nude mice (28). It has been posited that the interaction of the $\alpha3\beta1$ integrin with laminin, which promotes tumor cell migration and invasion, may be critical to this effect (28).

2) Immunoglobulin superfamily of cell adhesion molecules

Endothelial cells express several adhesion molecules belonging to the immunoglobulin superfamily, including members of the intercellular adhesion molecules (ICAMs), vascular-cell adhesion molecule (VCAM) and platelet-endothelial-cell adhesion molecule (PECAM) (29). These are essential in immune